



1 **Spatial gradients in soil-carbon character of a coastal forested floodplain are associated**  
2 **with abiotic features, but not microbial communities**

3

4 Aditi Sengupta<sup>1\*</sup>, Julia Indivero<sup>2</sup>, Cailene Gunn<sup>2</sup>, Malak M. Tfaily<sup>3,4</sup>, Rosalie K. Chu<sup>4</sup>, Jason  
5 Toyoda<sup>4</sup>, Vanessa L. Bailey<sup>1</sup>, Nicholas D. Ward<sup>2,5</sup>, James C. Stegen<sup>1</sup>

6 1. Biological Sciences Division, Pacific Northwest National Laboratory, PO Box 999  
7 MSIN: J4-18, Richland, WA 99352

8 2. Marine Sciences Laboratory, Pacific Northwest National Laboratory, 1529 West Sequim  
9 Bay Road, Sequim, WA 98382

10 3. Department of Soil, Water, and Environmental Sciences, University of Arizona, Tucson,  
11 AZ 85719

12 4. Environmental Molecular Sciences Laboratory, Pacific Northwest National Laboratory,  
13 Richland, WA 99352

14 5. School of Oceanography, University of Washington, Seattle, WA 98195

15 Correspondence to: aditi.sengupta@pnnl.gov

16

17

18

19

20

21

22

23

24



25 **Abstract**

26 Coastal terrestrial-aquatic interfaces (TAIs) are dynamic zones of biogeochemical cycling  
27 influenced by salinity gradients. However, there is significant heterogeneity in salinity influences  
28 on TAI soil biogeochemical function. This heterogeneity is perhaps related to unrecognized  
29 mechanisms associated with carbon (C) chemistry and microbial communities. To investigate  
30 this potential, we evaluated hypotheses associated with salinity-associated shifts in organic C  
31 thermodynamics, biochemical transformations, and heteroatom content in a first-order coastal  
32 watershed in the Olympic Peninsula of Washington state, USA. In contrast to our hypotheses,  
33 thermodynamic favorability of water soluble organic compounds in shallow soils decreased with  
34 increasing salinity, as did the number of inferred biochemical transformations and total  
35 heteroatom content. These patterns indicate lower microbial activity at higher salinity that is  
36 potentially constrained by accumulation of less favorable organic C. Furthermore, organic  
37 compounds appeared to be primarily marine/algal-derived in forested floodplain soils with more  
38 lipid-like and protein-like compounds, relative to upland soils that had more lignin-, tannin-, and  
39 carbohydrate-like compounds. Based on a recent simulation-based study, we further  
40 hypothesized a relationship between microbial community assembly processes and C chemistry.  
41 Null modelling revealed strong influences of dispersal limitation over microbial composition,  
42 which may be due to limited hydrologic connectivity within the clay-rich soils. Dispersal  
43 limitation indicated stochastically assembled communities, which was further reflected in the  
44 lack of an association between community assembly processes and C chemistry. This suggests a  
45 disconnect between microbial community composition and C biogeochemistry, thereby  
46 indicating that the salinity-associated gradient in C chemistry was driven by a combination of  
47 spatially-structured inputs and salinity-associated metabolic responses of microbial communities  
48 that were independent of community composition. We propose that impacts of salinity on coastal



49 soil biogeochemistry need to be understood in the context of C chemistry,  
50 hydrologic/depositional dynamics, and microbial physiology, while microbial composition may  
51 have less influence.

## 52 **1. Introduction**

53 The interface between terrestrial and aquatic ecosystems represent a dynamic and poorly  
54 understood component of the global carbon (C) cycle, particularly along the tidally-influenced  
55 reaches of coastal watersheds where terrestrial and marine biospheres intersect (Krauss et al.,  
56 2018; Neubauer et al., 2013; Tank et al., 2018; Ward et al., 2017b). Moreover, the nutrient cycles  
57 occurring at these terrestrial-aquatic interfaces (TAIs) influence locally important ecosystem  
58 services like contaminant fate and transport and water quality (Conrads and Darby, 2017; Vidon  
59 et al., 2010). While coastal soil C stocks are being increasingly quantified (Hinson et al., 2017;  
60 Holmquist et al., 2018; Krauss et al., 2018), the impact of tidally-driven salinity gradients on  
61 molecular level features of the soil-C pool and the processes driving soil organic matter (OM)  
62 cycling are poorly studied (Barry et al., 2018; Hoitink et al., 2009; Sawakuchi et al., 2017; Ward  
63 et al., 2017b), particularly in settings with low freshwater inputs that allows significant seawater  
64 intrusion compared to large river systems (Hoitink and Jay, 2016). Moreover, there is some  
65 indication that microbial diversity and composition impact soil C storage and mineralization  
66 (Mau et al., 2015; Trivedi et al., 2016). This points to the intriguing possibility that processes  
67 governing microbial community assembly may be associated with OM chemistry, but  
68 evaluations of such associations are lacking. This lack of mechanistic knowledge combined with  
69 significant ecosystem heterogeneity in biogeochemical function across salinity gradients (more  
70 below), highlights a need to understand how molecular-level processes vary with seawater  
71 exposure along coastal TAIs. Doing so will help enhance predictive models of TAI



72 biogeochemistry that can be potentially included in ecosystem models to more accurately  
73 represent the role of TAIs in the broader Earth system (U.S. DOE., 2017).  
74  
75 Modeling of coastal TAIs is currently impeded by poor knowledge of the mechanisms  
76 underlying salinity-driven variation in biogeochemical function of associated soils. Previous  
77 studies have evaluated function primarily as carbon dioxide (CO<sub>2</sub>) and methane (CH<sub>4</sub>) flux  
78 measurements from soil, and/or soil OM concentrations measured as bulk soil C, percent OM  
79 and porewater dissolved organic C (DOC) concentrations in large scale coastal plain river  
80 systems. Results from field-based natural salinity gradient studies, long-term field manipulations  
81 of salinity exposure, and lab-based incubation studies subjecting soils to varying levels of  
82 salinity broadly show the following trends: increases in CO<sub>2</sub> and decreases in CH<sub>4</sub> emissions in  
83 freshwater soils exposed to increasing salinity (Chambers et al., 2011, 2013, 2014; Liu et al.,  
84 2017; Marton et al., 2012; Neubauer et al., 2013; Steinmuller and Chambers, 2018; Weston et al.,  
85 2006, 2011), and decreases in CO<sub>2</sub> and CH<sub>4</sub> emissions from soils with a natural history of being  
86 exposed to saline environment when exposed to elevated salinity (Chambers et al., 2013; Herbert  
87 et al., 2018; Neubauer et al., 2005, 2013; Weston et al., 2014) (also see Table S1). Two  
88 exceptions have been observed where CO<sub>2</sub> emissions decreased in historically freshwater coastal  
89 wetland soils exposed to seawater (Ardón et al., 2018; Herbert et al., 2018). These observations  
90 suggest that microbial activity usually increases with salinity in soils that were not previously  
91 exposed to saline conditions, while simultaneously indicating reduced microbial activity with  
92 increasing salinity in soils that have a historical exposure to elevated salinity. In contrast to  
93 relatively consistent responses of gas fluxes to changes in salinity, there are strong  
94 inconsistencies in DOC responses, including no change (Weston et al., 2006, 2011, 2014),



95 increased DOC (Chambers et al., 2014; Tzortziou et al., 2011), and decreased DOC (Ardón et al.,  
96 2016, 2018; Liu et al., 2017; Yang et al., 2018) with increasing salinity.  
97  
98 Relatively consistent gas flux responses combined with inconsistent DOC responses of soils  
99 exposed to elevated salinity suggest at least a partial decoupling between microbially driven  
100 biogeochemical rates and the concentration of DOC. This apparent decoupling between the size  
101 of the C pool and microbial activity suggests that C biogeochemistry is influenced by salinity-  
102 exposure history, which in turn influences nutrient resources available to soil microbial  
103 communities. Specifically, any systematic shifts in soil organic carbon (SOC) chemistry profiles  
104 that occur along natural salinity gradients (Bischoff et al., 2018; Neubauer et al., 2013), which  
105 cannot be observed with bulk C measurements may result in unpredictable carbon fluxes.  
106 Moreover, bulk C content can show no change across gradients of salinity (Neubauer et al.,  
107 2013) and may fail to capture an integrated view of microbial-activity driven C cycling dynamics  
108 at TAIs. In contrast, detailed molecular-level evaluation of SOC composition can provide a more  
109 mechanistic view of OC transformations, relative to bulk measures of C content or gas flux  
110 measurements. Analyses of specific chemical biomarkers such as lignin phenols, amino acids,  
111 and lipids have been used in soils, sediments, and water to quantitatively evaluate the provenance  
112 of terrestrial-derived OM (Hedges et al., 1997), the reactivity of OM as it travels through a soil  
113 column (Shen et al., 2015), and microbial community composition (Langer and Rinklebe, 2009),  
114 respectively. While biomarkers provide quantitative details on OC cycling, they generally  
115 represent a small fraction of the total OM pool, thus, non-targeted approaches such as analysis of  
116 thousands of peaks via Fourier Transform Ion Cyclotron Resonance Mass Spectrometry (FTICR-  
117 MS) have become increasingly widespread for determining molecular-level organic compound  
118 signatures (Rivas-Ubach et al., 2018) across a variety of terrestrial (Bailey et al., 2017; Simon et



119 al., 2018), aquatic/marine (Lechtenfeld et al., 2015), and transitional settings such as hyporheic  
120 zones (Graham et al., 2017a) and river-ocean gradients (Medeiros et al., 2015).  
121  
122 Despite its potential importance, a detailed understanding of the characteristics of soil organic  
123 compounds (Zark and Dittmar, 2018) and their association with microbial communities in  
124 coastal TAIs is currently not available. However, starting with an assumption of increases in  
125 microbial activity with increasing salinity (Nyman and Delaune, 1991; Smith et al., 1983;  
126 Tzortziou et al., 2011) provides a series of expectations. First, it is generally expected that  
127 microbes preferentially degrade compounds with higher nominal oxidation states (NOSC) or  
128 lower Gibbs Free Energy ( $\Delta G^0_{\text{Cox}}$ ) due to greater thermodynamic favorability (Boye et al., 2017;  
129 Ward et al., 2017a), although factors such as redox state, mineral associations, and microbial  
130 community composition can alter this generality (Schmidt et al., 2011). The basic assumption  
131 that OM reactivity follows NOSC leads to the expectation that the average  $\Delta G^0_{\text{Cox}}$  of the  
132 compounds in the resource environment will increase with increasing salinity as organic  
133 compounds with greater thermodynamic favorability are preferentially depleted (LaRowe and  
134 Van Cappellen, 2011). Second, actively growing microbial communities are known to enhance  
135 biochemical transformations and generate heteroatom containing organic molecules [sulfur (S),  
136 nitrogen (N) and phosphorus (P)] (Guillemette et al., 2018; Koch et al., 2014; Ksionzek et al.,  
137 2016); therefore greater heteroatom content and more biochemical transformations are expected  
138 with increasing salinity. Third, studies have also shown that microorganisms adapt to saline  
139 conditions through the production or sequestration of osmolytes (Gouffi et al., 1999; Roberts,  
140 2005; Sleator and Hill, 2002), a strategy that requires organic N mining. This suggests a  
141 potential increase in N-containing biochemical transformation with increasing salinity. Fourth,  
142 soil OM in saturated environments like floodplains are expected to be less oxygenated and can



143 also receive deposition of suspended sediments during flooding, both of which may result in a  
144 greater abundance of marine/algal derived OM exhibiting low oxygen to carbon (O/C) and high  
145 hydrogen to carbon (H/C) ratio as compared to upland soils (Seidel et al., 2016; Tfaily et al.,  
146 2014; Ward et al., 2019b). We therefore expect a greater relative abundance of lipids and  
147 proteins and less lignin and tannin compounds in the floodplain soils, relative to upland (i.e.,  
148 drained) soil.

149

150 While we expect systematic shifts in C chemistry across landscape scale salinity gradients, an  
151 open question is the degree to which C chemistry is associated with ecological assembly  
152 processes governing microbial communities. Soil microorganisms transform soil C, but there is  
153 limited evidence of direct links between microbial community assembly processes and  
154 molecular-level soil C chemistry (Kubartová et al., 2015; Rocca et al., 2015; Trivedi et al., 2016;  
155 van der Wal et al., 2015). Assembly processes, broadly divided into deterministic (selective) and  
156 stochastic (random) factors, function over space and time to structure microbial communities,  
157 which in turn mediate biogeochemical cycles (Graham et al., 2016, 2017b; Nemergut et al.,  
158 2013a; Stegen et al., 2015). These processes can be inferred from phylogenetic distances among  
159 microbial taxa using ecological null models, which have been widely employed to understand  
160 community assembly processes in subsurface microbial ecology (Caruso et al., 2011; Dini-  
161 Andreote et al., 2015; Graham et al., 2017a, 2018; Stegen et al., 2012). Furthermore, a recent  
162 study used ecological simulation modeling to show that environments experiencing increasing  
163 rates of dispersal processes are linked to reduced biogeochemical functioning (Graham and Fine,  
164 2008). This leads to the hypothesis that the influence of deterministic selection will progressively  
165 increase with salinity-driven increases in microbial activity.

166



167 The objective of the current study was to test the following hypotheses in a coastal forested  
168 floodplain and adjacent upland forest: (i) the overall Gibbs Free Energy of organic compounds  
169 will increase with increasing salinity; (ii) biochemical transformations, heteroatom content, and  
170 N-containing biochemical transformation will increase with increasing salinity; (iii) the lipid and  
171 protein compound classes will be prevalent in the floodplain soils compared to upland soils in  
172 which lignin- and tannin-type molecules will dominate; and (iv) microbial community assembly  
173 processes will be increasingly deterministic as salinity increases. The chemical forms of C in  
174 these soils were characterized using FTICR-MS. We also employed ecological null model  
175 analysis to evaluate the relationship between C chemistry and the influences of assembly  
176 processes on microbial communities. Based on our results, we propose a conceptual model of  
177 organic C processing in a coastal forested floodplain in which landscape-scale gradients in C  
178 chemistry are driven by a combination of spatially-structured inputs and salinity-associated  
179 metabolic responses of microbial communities that are independent of community composition.

180

## 181 **2. Materials and Methods:**

### 182 **2.1 Site Information and Soil Sampling**

183 Soils along a coastal watershed draining a small first order stream, Beaver Creek, in the  
184 Washington coast were selected for this study. Beaver Creek is a tributary of Johns River and  
185 experiences a high tidal range of up to 2.5 m that extends midway up the first-order stream's  
186 channel and inundates the landscape in its floodplains. The confluence of Beaver Creek and  
187 Johns River is roughly 2.5 km upstream of the Grays Harbor estuary and 14.5 km from the  
188 Pacific Ocean, and experiences variable exposure to saline waters at high tide (Fig. 1). Surface  
189 water salinity near Beaver Creek's confluence ranges from 0 psu at low tide to 30 psu at high  
190 tide during dry periods (Ward, unpublished). Tidal exchange to Beaver Creek was restored after



191 2014 when a culvert near the creek's confluence with Johns River was removed (Washington  
192 Department of Fish and Wildlife, 2019). Due to the minimal past tidal exchange, the floodplain  
193 is dominated by gymnosperm trees (*Picea sitchensis*) that are rapidly dying since the culvert  
194 removal (Ward et al., 2019a). The headwaters (before the river channel forms) is a sparsely  
195 forested, perennially inundated freshwater wetland with tidal exchange blocked by a beaver dam,  
196 followed downstream by a densely forested setting along the river channel. Towards Beaver  
197 Creek's confluence salt tolerant grasses such as *Agrostis stolonifera* become the most dominant  
198 land cover as forest cover becomes more sparse. The watershed's hillslope/uplands is dominated  
199 by *Tsuga heterophylla* trees, but *Picea sitchensis* are also present.

200

201 Two sampling transects perpendicular to the river along the up/downstream salinity gradient  
202 were established and represent a high salt exposure site close to the culvert breach location and a  
203 moderate salt exposure site upstream of the high salt exposure site. These transects represent a  
204 coastal forested wetland with brackish (semi-salty) groundwater and consisted of three terrestrial  
205 sampling points at each transect extending from the riparian zone to the beginning of the steep  
206 upslope. An additional soil sampling point ~20m uphill from the moderate salt exposure site  
207 transect served as a purely terrestrial upland endmember. The floodplain transects represented  
208 hydric soils classified as Ocosta silty clay loam while the upland site was a well-drained Mopang  
209 silt loam. The transects experience periodic inundation episodes which result in surface pooling  
210 of tidal water.

211

212 Soil samples were collected in triplicate at each of the seven locations (Fig. 1) [BC2, BC3, and  
213 BC4 at the high-salt exposure transect, locations BC12, BC13, BC14 at the moderate salt  
214 exposure transect, and BC15 as upland site]. The high-salt exposure transect was 230 m from the



215 moderately saline transect (0.6 km from the confluence of Beaver Creek with Johns River), and  
216 each site at the transect was ~25 m apart from the next. For data comparison's sake, we classify  
217 BC2, BC3, BC12, and BC13 as **floodplain** sites while BC4 and BC14 are further **inland** and ~75  
218 m away from the creek at the base of the densely wooded hillslope. Soil samples for molecular  
219 characterization studies were collected at two depths—shallow (10 cm) and deep (19-30 cm).  
220 Samples were collected from the face of soil pits using custom mini-corers, placed into sterile  
221 amber glass vials, purged with N<sub>2</sub> to maintain anaerobic conditions, frozen in the field within an  
222 hour at -20 °C, and stored at -80 °C on return to the lab. Bulk samples were collected for soil  
223 physicochemical characterization including texture classification with hydrometer method after  
224 organic matter removal, dry combustion with direct measure of total C, nitrogen (N) and sulfur  
225 (S) by Elementar Macro Cube, plant-available N as ammonium-nitrogen (NH<sub>4</sub>-N) and nitrate-  
226 nitrogen (NO<sub>3</sub>-N) with 2M KCl quantified on Lachat as colorimetric reaction, pH, specific  
227 conductivity, gravimetric water content, bulk density, and porosity. Molecular characterization  
228 included ultra-high resolution C characterization using FTICR-MS and microbial community  
229 assembly analyses using amplicon-based 16S rRNA gene sequencing.

230

## 231 **2.2 FTICR-MS solvent extraction and data acquisition**

232 Soil organic compounds were extracted using a sequential extraction protocol with polar {water  
233 (H<sub>2</sub>O)} and non-polar {chloroform (CHCl<sub>3</sub>) and methanol (CH<sub>3</sub>OH)} solvents per standardized  
234 protocols (Graham et al., 2017a; Tfaily et al., 2015, 2017). Briefly, extracts were prepared by  
235 adding 5 ml of MilliQ H<sub>2</sub>O to 5 g of each of the replicate samples in sterile polypropylene  
236 centrifuge tubes (Genesee Scientific, San Diego, USA) suitable for organic solvent extractions  
237 and shaking for 2 h on a Thermo Scientific LP Vortex Mixer. Samples were removed from the  
238 shaker and centrifuged for 5 minutes at 6000 rpm, and the supernatant was removed into a fresh



239 centrifuge tube. This step was repeated two more times, with the 15 ml supernatant pooled for  
240 each sample and stored at -80 °C until further processing. Next, Folch extraction with CHCl<sub>3</sub> and  
241 CH<sub>3</sub>OH was performed for each soil pellet left over from the water extraction. Folch extraction  
242 entailed adding 2 ml CH<sub>3</sub>OH, vortexing for 5 seconds, adding 4 ml CHCl<sub>3</sub>, vortexing for 5  
243 seconds, followed by of 0.25 ml of MilliQ H<sub>2</sub>O. The samples were shaken for 1 hr and another  
244 1.25 ml MilliQ H<sub>2</sub>O was added and left overnight at 4 °C to obtain bi-layer separation of upper  
245 (polar) layer and the lower (non-polar) layer. The extracts were stored in glass vials at -20 °C  
246 until ready to be used. The water soluble organic carbon (WSOC) fraction was further purified  
247 using a sequential phase extraction protocol to remove salts as per Dittmar et al., 2008. For the  
248 purpose of this study, purified WSOC and CHCl<sub>3</sub> fractions were used. The extracts were  
249 injected into a 12 Tesla Bruker Solarix FTICR-MS located at Environmental Molecular Sciences  
250 Laboratory (EMSL) in Richland, WA, USA. Detailed methods for instrument calibration,  
251 experimental conditions, and data acquisition are provided in Graham et al., 2017a and Tfaily et  
252 al., 2017.

253

### 254 **2.3 FTICR-MS Data Processing**

255 One hundred forty-four individual scans were averaged for each sample and internally calibrated  
256 using an organic matter homologous series separated by 14 Da (-CH<sub>2</sub> groups). The mass  
257 measurement accuracy was less than 1 ppm for singly charged ions across a broad m/z range  
258 (100 - 900 m/z). Data Analysis software (Bruker Daltonik version 4.2) was used to convert raw  
259 spectra to a list of m/z values applying FTMS peak picker module with a signal-to-noise ratio  
260 (S/N) threshold set to 7 and absolute intensity threshold to the default value of 100. Chemical  
261 formulae were then assigned using in-house software following the Compound Identification  
262 Algorithm, proposed by Kujawinski and Behn (2006), modified by Minor et al. (2012), and



263 described in Tolić et al. (2017). Peaks below 200 and above 900 were dropped to select only for  
264 calibrated and assigned peaks. Chemical formulae were assigned based on the following criteria:  
265  $S/N > 7$ , and mass measurement error  $< 0.5$  ppm, taking into consideration the presence of C, H,  
266 O, N, S, P, and excluding other elements. Detected peaks and associated molecular formula were  
267 uploaded to the in-house pipeline FTICR R Exploratory Data Analysis (FREDA) to obtain: (i)  
268 NOSC values from elemental composition of the organic compounds (Koch and Dittmar, 2006,  
269 2016), (ii) thermodynamic favorability of the compounds calculated as Gibbs Free Energy for the  
270 oxidation half reactions of the organic compounds ( $\Delta G^0_{\text{cox}}$ ) based on the equation  $\Delta G^0_{\text{cox}} =$   
271  $60.3 - 28.5 * \text{NOSC}$  (LaRowe and Van Cappellen, 2011), where a higher  $\Delta G^0_{\text{cox}}$  indicates a less  
272 thermodynamically favorable species than a lower value (LaRowe and Van Cappellen, 2011),  
273 (iii) abundance of compounds grouped into elemental groups (CHO, CHOS, CHOP, CHNOS,  
274 CHNO, CHNOP, CHOSP, and CHNOSP), and (iv) abundance of compound classes  
275 (carbohydrate-, lipid-, protein-, amino sugar-, lignin-, tannin-, condensed hydrocarbon-, and  
276 unsaturated hydrocarbon-like) based on molar H:C and O:C ratios of the compounds (Bailey et  
277 al., 2017).

278

279 Biochemical transformations potentially occurring in each sample were inferred from the  
280 FTICR-MS data by comparing mass differences in peaks within each sample to precise mass  
281 differences for commonly observed biochemical transformations (Breitling et al., 2006; Stegen  
282 et al., 2018b). The ultra-high mass accuracy of FTICR-MS allows precise mass differences to be  
283 counted for the number of times each transformation was observed within each sample. Briefly,  
284 the mass difference between  $m/z$  peaks extracted from each spectrum were compared to  
285 commonly observed mass differences associated with 92 common biochemical transformations



286 provided in previous publications (Graham et al., 2017a; Stegen et al., 2018c). All possible  
287 pairwise mass differences were calculated within each extraction type for each sample. For  
288 example, a mass difference of 97.05 corresponds to a gain or loss of the amino acid proline,  
289 while a difference of 43.98 corresponds to the gain or loss of a carboxylate molecule.

290

## 291 **2.4 Ecological Modeling**

292 Null modeling was used to estimate influences of ecological processes on microbial community  
293 composition from rarefied (10000) 16S rRNA amplicon-dependent microbial community  
294 composition and phylogenetic relatedness. The extraction, purification, and sequencing of soil  
295 microbial DNA were performed according to published protocol (Bottos et al., 2018). Sequence  
296 pre-processing, operational taxonomic unit (OTU) table construction and phylogenetic tree  
297 building were performed using an in-house pipeline, HUNDO (Brown et al., 2018). Null  
298 modeling was performed as described previously (Stegen et al., 2013, 2015) with a total of 35  
299 samples to estimate relative influences of deterministic and stochastic selection processes.

300 Briefly, samples that passed quality control and rarefaction threshold were evaluated for pairwise  
301 phylogenetic turnover between communities, calculated as the difference between the mean-  
302 nearest-taxon-distance ( $\beta$ MNTD) metric and mean of the null distribution in units of standard  
303 deviation. The difference was significant if the  $\beta$ -nearest taxon index ( $\beta$ NTI)  $> 2$  or  $< -2$   
304 signifying variable or homogenous selection, respectively.

305 Comparisons within the null distribution ( $2 > \beta$ NTI  $> -2$ ) represent stochastic processes including  
306 homogenizing dispersal and dispersal limitation or undominated processes. These processes were  
307 evaluated using the Raup-Crick metric extended to account for species relative abundances  
308 ( $RC_{bray}$ ) (Stegen et al., 2013, 2015). Homogenizing dispersal was inferred if deviations were  
309  $2 > \beta$ NTI  $> -2$  and  $RC_{bray} < -0.95$ , while deviations  $2 > \beta$ NTI  $> -2$  and  $RC_{bray} > 0.95$  suggested dispersal



310 limitation. Undominated processes were represented by comparison within the null distribution  
311 of both metrics ( $2 > \beta_{\text{NTI}} > -2$  and  $0.95 > \text{RC}_{\text{bray}} > -0.95$ ). Raw sequences are archived at NCBI  
312 (BioProject PRJNA541992) with reviewer link  
313 (<https://dataview.ncbi.nlm.nih.gov/object/PRJNA541992?reviewer=b55qu29emsinvk3udb2rmuf>  
314 fqh).

315

## 316 **2.5 Statistical Methods**

317 Samples were separately analyzed for WSOC and  $\text{CHCl}_3$  fractions. Within each solvent fraction,  
318 samples were grouped into shallow or deep depths. FTICR-MS dependent metrics including  
319  $\Delta G^0_{\text{Cox}}$ , and relative abundance of compound classes, total transformations, nitrogen-containing  
320 transformations, and organic nitrogen containing compounds were regressed against specific  
321 conductivity. Regressions were considered significant if  $R^2 \geq 0.50$  and  $p \leq 0.05$ . The  
322 transformation profiles were also regressed with the community assembly processes to determine  
323 the relationship between deterministic/stochastic processes and organic compound  
324 transformations. Mantel tests were used to evaluate similarity between BNTI matrix and  
325 Sorensen matrix of peak presence/absence. The Sorensen distance matrices of WSOC and  $\text{CHCl}_3$   
326 peaks were regressed against measured variables (soil physicochemical properties) and  
327 community assembly process-variables to determine correlations. Finally, a redundancy analysis  
328 –based stepwise model building with forward model choice was performed to determine  
329 variation in the Hellinger-transformed water-fraction peaks and  $\text{CHCl}_3$  fraction peaks as  
330 explained by explanatory variables (which included measured soil variables, modeled  
331 community assembly variables, and categorical variables depth and location). All statistical  
332 analyses were performed in the statistical computing language R version 3.5.3 (R Development  
333 Core Team, 2019).



334

### 335 3. Results

336 **3.1 Soil characterization.** The percent of total soil C (%C) in the shallow soils ( $26.3 \pm 8.3\%$ )  
337 was higher than the deeper soils ( $4.0 \pm 1.3\%$ ) for the lowland soils (i.e. “floodplain” and “inland”  
338 sites), while the upland site had an average %C of  $7.4 \pm 0.27\%$  at 10 cm and  $2.13 \pm 0.06\%$  at 30  
339 cm (Table S2). No significant relation was observed between %C in the shallow inland and  
340 floodplain soils along the salinity gradient. The percent of total soil N (%N) of the shallow soils  
341 were higher ( $1.5 \pm 0.40\%$ ) than the deeper soils ( $0.4 \pm 0.08\%$ ) for the lowland soils and co-varied  
342 with %C ( $r^2=0.95$ ). The pH of all soils were acidic ( $5.64 \pm 0.70$ ). The concentrations of  $\text{NH}_4\text{-N}$   
343 and  $\text{NO}_3\text{-N}$  showed a consistent trend where  $\text{NH}_4\text{-N}$  was 1-2 orders of magnitude higher than  
344  $\text{NO}_3\text{-N}$  in all samples. The specific conductivity (used as a measurement of salinity in this study)  
345 of the shallow soils ranged from 206-866 ( $\pm 12$ )  $\mu\text{S cm}^{-1}$  in the lowland soils to  $43 \pm 5$   $\mu\text{S cm}^{-1}$  in  
346 the terrestrial end-member site. The deep soils exhibited specific conductivity ranging from to  
347 148-524 ( $\pm 11$ )  $\mu\text{S cm}^{-1}$  in the lowland soils to  $29.2 \pm 8$   $\mu\text{S cm}^{-1}$  in the terrestrial end-member site.  
348 Texture analysis revealed a broad range of sand (4.1 – 40 %), silt (21.4 – 57.9%), and clay (28.6  
349 – 64.8%) fractions.

350

351 **3.2 Thermodynamics, compound classes, and elemental composition.** The calculated  $\Delta G^0_{\text{Cox}}$   
352 WSOC (Table S3) in shallow soils was consistent with our hypothesis of decreasing  
353 thermodynamic favorability with increasing conductivity. Average  $\Delta G^0_{\text{Cox}}$  ranged from 53-71 kJ  
354  $\text{mol C}^{-1}$  ( $R^2= 0.78$ ,  $p < 0.00001$ ), while no significant relationship between  $\Delta G^0_{\text{Cox}}$  and specific  
355 conductivity was observed for WSOC fraction in the deeper soils (averaging 51-54 kJ  $\text{mol C}^{-1}$ )  
356 for the floodplain and inland samples (Fig. 2). The upland site had significantly higher average  
357  $\Delta G^0_{\text{Cox}}$  (67-70 kJ  $\text{mol C}^{-1}$ ) than the soils near the lowland. The  $\Delta G^0_{\text{Cox}}$  ( $\text{CHCl}_3$ ) at both depths



358 (Table S4) was higher than the water fractions (ranging between 96-105 kJ mol C<sup>-1</sup>) but did not  
359 show significant relationship with respect to specific conductivity.  
360  
361 Peak profiles for each solvent extraction showed distinct compound classes in the van Krevelen  
362 space, with peaks assigned to specific compound classes according to rules outlined in Kim et  
363 al., 2003 and modified by Bailey et al., 2017. The WSOC fraction was dominated by compounds  
364 classified as protein-, amino sugar-, lignin-, condensed hydrocarbon-, carbohydrate-, and tannin-  
365 like compounds (Table 1), while the CHCl<sub>3</sub> fraction had relative high abundances (75% and  
366 higher) of lipid-like compounds (data not shown). A modest percentage of peaks (11-17%) did  
367 not have classes assigned. Unique and common peaks extracted in the WSOC fraction in samples  
368 grouped according to their landscape position and depth [four sites in the floodplain (BC2, BC3,  
369 BC12, and BC13), two sites inland (BC4 and BC14), and one upland site (BC15)] are  
370 represented as H/C to O/C ratio of the compounds ( $p = 0.05$ ) in Fig. S1.  
371 The shallow WSOC in the floodplain had greater relative abundance of unique lipid (28%)- and  
372 protein (25%)-like compounds with relatively high H:C and low O:C ratios as compared to the  
373 upland site (BC15), which had an 31%, 30%, and 19% unique peaks representing lignin-,  
374 tannin-, and carbohydrate-like compounds respectively. About 23% of peaks were common in  
375 both groups, including lignin- and condensed hydrocarbon-like compounds (Fig. S1a). Between  
376 the floodplain and the inland samples, high H:C and low O:C ratios representing 47% lipid-,  
377 38% protein-, and 22% amino sugar-like peaks were uniquely present in the floodplain samples  
378 (Fig. S1b). The inland shallow soils had 19% unique higher H:C peaks representing condensed  
379 hydrocarbon-like compounds compared to 1.2% in the upland soil, though most of the  
380 compound classes were observed at both locations (Fig. S1c). Linear regression with specific  
381 conductivity profiles showed significant positive correlation with amino sugar-, protein-, lipid-,



382 and unsaturated hydrocarbon-like compounds, while condensed hydrocarbon-like compounds  
383 were significantly negatively correlated (Table S5)

384

385 For the deep soils, the upland site had 32% unique peaks with relatively high H:C ratios and low  
386 O:C ratios commonly associated with unsaturated hydrocarbon-like compounds, as compared to  
387 the 0.7% in the floodplain which had higher prevalence of unique peaks representing condensed  
388 hydrocarbon (36%)-, and tannin-like (35%) compounds (Table 1, Fig. S1d). The floodplain vs  
389 inland samples had thrice as many unique peaks with high H:C and low O:C ratios representing  
390 lipid-like compounds in the floodplain samples. Comparisons between inland and upland end-  
391 member samples revealed 43% and 37% unique peaks representing low H:C and high O: C ratio  
392 hydrocarbon- and tannin-like compounds respectively in inland samples, while 32%, 14% 9%,  
393 and 12% of unique peaks were matched to unsaturated hydrocarbon-, lipid-, protein-, and amino  
394 sugar-like compounds respectively in the latter (Table 1, Fig. S1e, f). No significant relationship  
395 was observed with specific conductivity (Table S5). For the  $\text{CHCl}_3$  fraction, peaks of lipid-like  
396 and unsaturated hydrocarbon-like compounds were observed to be common in all samples (data  
397 not shown) and regressions against specific conductivity were not significant for the compound  
398 classes.

399

400 Compositional differences of the organic compounds showed variable heteroatom abundances,  
401 with cumulative heteroatom abundance decreasing with increasing salinity ( $R^2=0.43$ ,  $p = 0.009$ )  
402 for shallow fraction of the WSOC. For the WSOC fraction, heteroatom abundance of CHOP ( $R^2$   
403 = 0.61) and CHNOP ( $R^2 = 0.50$ ) containing compounds was consistent with our hypothesis and  
404 significantly ( $p < 0.01$ ) increased, while CHNOS ( $R^2 = 0.66$ ), and CHNOSP ( $R^2 = 0.62$ )  
405 abundances were inconsistent with our hypothesis and significantly decreased with increasing



406 specific conductivity. The elemental composition of the WSOC compounds for deep soils did not  
407 show any significant trend with respect to conductivity. For the  $\text{CHCl}_3$  fraction, relative  
408 abundance of CHNOP in the shallow soils significantly decreased with specific conductivity ( $R^2$   
409 = 0.57,  $p < 0.01$ ).

410

411 **3.3 Transformation profiles.** In contrast to our expectations, the number of transformations  
412 decreased with increasing salinity in the water fraction of shallow soils ( $R^2 = 0.60$ ,  $p < 0.01$ ) (Fig.  
413 3a, Table S3). We also evaluated N-containing transformations and the abundance of N-  
414 containing compounds in the system. Total nitrogen-containing transformations also decreased  
415 significantly with conductivity but the correlation was not as strong ( $R^2 = 0.40$ ,  $p < 0.01$ ). Total N  
416 containing compounds (Fig. 3b, Table S3) as well as their relative abundance decreased  
417 significantly ( $R^2 = 0.74$ ,  $p < 0.01$ ), with increasing conductivity in the shallow soils for water  
418 fraction.

419

#### 420 **3.4 Ecological processes impacting community composition**

421 Null modeling revealed that community assembly processes were influenced by variable  
422 selection ( $\beta\text{NTI} > 2$ ), homogenous selection ( $\beta\text{NTI} < -2$ ), dispersal limitation ( $2 > \beta\text{NTI} > -2$  and  
423  $\text{RC}_{\text{bray}} > 0.95$ ), homogenizing dispersal ( $2 > \beta\text{NTI} > -2$  and  $\text{RC}_{\text{bray}} < -0.95$ ), and undominated  
424 processes ( $2 > \beta\text{NTI} > -2$  and  $0.95 > \text{RC}_{\text{bray}} > -0.95$ ) (Fig. 4). Dispersal limitation had the greatest  
425 influence, responsible for 54% of the variation in community composition. The lowest signal  
426 was for homogenizing dispersal (1%), and the signal for homogenous selection (23%) was higher  
427 than variable selection (9%). Together, deterministic processes (variable selection plus  
428 homogeneous selection) were responsible for 32% of the variation in community composition,  
429 with 55% contributed by stochastic processes (dispersal limitation plus homogenizing dispersal).



430 Variation not accounted by dispersal or selection (i.e., influenced by a mixture of processes)  
431 accounted for the remaining signal (23%). Consistent with influences from both stochastic and  
432 deterministic processes,  $\beta$ NTI relationships with environmental variables were significant ( $p <$   
433  $0.05$  by Mantel test), but relatively weak ( $r=0.46$  for pH and  $r=0.31$  for specific conductivity)  
434 (Fig. S2).

435

436 To evaluate associations between microbial community assembly processes and chemistry,  
437 process estimates were regressed against features of the organic C profiles. Deterministic  
438 processes decreased (Fig S3a) while community assembly processes influenced by non-  
439 deterministic processes increased with increasing number of transformations of organic  
440 compounds (Fig. S3b), although no strong relationships were observed between assembly  
441 processes and transformations ( $p = 0.027$ ,  $R^2 = 0.11$  for deterministic/non-deterministic  
442 processes,  $p = 0.475$ ,  $R^2 = 0.015$  for variable selection,  $p = 0.054$ ,  $R^2 = 0.10$  for homogenous  
443 selection,  $p = 0.514$ ,  $R^2 = 0.013$  for dispersal limitation, and  $p = 0.627$ ,  $R^2 = 0.007$  for  
444 homogenizing dispersal). No significant relationships were observed between assembly  
445 processes and the number of N-containing transformations. Sorensen dissimilarity values based  
446 on the detected FTICR peaks for the water fraction were correlated with distance matrices of  
447 measured environmental variables and estimates of community assembly processes. Weak  
448 positive correlations were observed with  $\text{NH}_4\text{-N}$  ( $r = 0.28$ ), pH ( $r = 0.27$ ), specific conductivity ( $r$   
449  $= 0.41$ ),  $\text{NO}_3\text{-N}$ , silt, and clay ( $r = 0.30$ ) while for the  $\text{CHCl}_3$  fraction, weak positive correlations  
450 were observed with specific conductivity and  $\text{NO}_3\text{-N}$  ( $r = 0.26$ ) (Fig. S4). A Mantel test of  
451 FTICR Sorensen dissimilarity vs  $\beta$ NTI values yielded a significant relationship ( $r = 0.213$ ,  $p =$   
452  $0.003$ ) for water fraction but not for  $\text{CHCl}_3$  fraction ( $r=0.076$ ,  $p = 0.152$ ). The stepwise model  
453 building yielded a combination of five variables that were weakly associated with the



454 composition of water fraction peaks ( $p=0.026$ , adj.  $R^2 = 0.217$ ), including sand, dispersal  
455 limitation,  $\text{NH}_4\text{-N}$  concentration, specific conductivity, and location. The model explaining  
456 variation in the composition of  $\text{CHCl}_3$  fraction peaks was non-significant ( $p = 0.1$ , adj.  $R^2 =$   
457 0.05).

458

#### 459 **4. DISCUSSION**

460 Sea level rise is increasing the inland extent of tides and exacerbating storm surge, resulting in  
461 greater salinity intrusion and altered ecosystem behavior across coastal TAIs (Conrads and  
462 Darby, 2017; Ensign and Noe, 2018; Langston et al., 2017; McCarthy et al., 2018; Neubauer et  
463 al., 2013). Site-driven variations in the responses of bulk soil biogeochemical processes (i.e., gas  
464 flux and DOC release) to elevated salinity suggests potentially important influences of  
465 underlying features such as C chemistry and microbial communities. To provide a foundation for  
466 understanding the role of C chemistry and microbial communities on biogeochemical cycling in  
467 coastal soils, we evaluated associations among a landscape-scale soil salinity gradient,  
468 molecular-level soil carbon chemistry, and microbial community assembly processes in order to  
469 ultimately inform future improvements for predictive models. In soils associated with a coastal  
470 first-order drainage basin, we observed salinity-associated gradients in soil organic carbon  
471 character that were not associated with microbial community assembly processes. Our results are  
472 consistent with C chemistry being driven by a combination of spatially-structured inputs and  
473 salinity-associated metabolic responses of microbial communities that are independent of  
474 microbial community composition.

475

#### 476 **4.1 Molecular characterization reveals chemical gradients not seen in the bulk C pool**



477 The systematic shifts observed in the molecular signatures compared to non-significant changes  
478 in bulk C chemistry shows that molecular-level investigations are particularly relevant to  
479 process-based resolution of C biogeochemistry. The absence of bulk C signals mimicking  
480 molecular C signals parallel studies indicating rapid change in molecular constituents of the soil  
481 C pool with no change in gross C content (Graham et al., 2018; Reynolds et al., 2018). A faster  
482 turnover time of C has been observed in microbial biomass as compared to bulk soil organic  
483 matter (Kramer and Gleixner, 2008), which is likely to impact microbe-mediated biochemical C  
484 transformations and lead to chemically complex heterogeneous C signatures likely to be missed  
485 in bulk analysis (Tfaily et al., 2015). The systematic C character shifts exhibited by samples at  
486 the shallow depth suggests that organic C compound pools in shallower soil depths are sensitive  
487 to salinity gradients while deeper depth signatures do not vary systematically across the  
488 landscape. The landscape gradient observed in the shallow soils is likely influenced by a  
489 combination of reduced litterfall from the recently suffering trees, changing understory  
490 vegetation, and algae-rich particulate OM deposition during inundation events that presumably  
491 initiated after the recent culvert removal. In contrast, the deeper soil depths were more similar to  
492 older organo-mineral complexed C in terrestrial soils across various ecosystems and land uses  
493 (Conant et al., 2011; Dungait et al., 2012; Jobbágy and Jackson, 2000; Kramer and Gleixner,  
494 2006, 2008). The lack of any systematic gradients in the mineral-associated soil C provides  
495 further evidence in support of these interpretations, in addition to previous studies showing  
496 mineral-associated soil C to be less responsive to environmental forcings, relative to water  
497 soluble C (Reynolds et al., 2018).

498

#### 499 **4.2 Decreases in organic C thermodynamic favorability may restrict microbial activity**



500 Consistent with our first hypothesis, systematic changes in soil organic C character were  
501 observed with thermodynamically less favorable C present at high salinity in shallow soils. This  
502 gradient was expected to emerge from increased microbial activity at higher salinity leaving  
503 behind less favorable organic C. However, decreases in the number of inferred biochemical  
504 transformations and heteroatom abundances with increasing salinity suggests that microbial  
505 activity decreased with increasing salinity. While difficult to infer direction of causality, these  
506 patterns suggest that less favorable C at higher salinities may constrain microbial activity,  
507 leading to fewer biochemical transformations of the organic C. Thermodynamic limitation of  
508 organic C transformation is likely due to anaerobic conditions (LaRowe and Van Cappellen,  
509 2011), which are indicated by high-moisture content of soils, high  $\text{NH}_4\text{-N}$ , and low  $\text{NO}_3\text{-N}$ .  
510 Anaerobic conditions restrict oxidation of C compounds based on thermodynamic properties  
511 (i.e., NOSC and  $\Delta G^0_{\text{Cox}}$ ) (Boye et al., 2017), and our data suggest that this has the potential to  
512 lead to lower microbial activity in conditions with less favorable organic C.

#### 513 **4.3 Compound class landscape gradients suggest influences of spatially structured inputs**

514 Similar to patterns in C thermodynamic favorability, C compound classes showed significant  
515 heterogeneity in shallow soils but had conserved characteristics in deeper soils. The lipid-like  
516 peaks observed in the shallow floodplain samples suggest marine-associated algal-derived lipid  
517 organic matter similar to results observed by Ward et al., 2019 in a coastal wetland setting. In  
518 contrast, lignin-like signatures in the upland site suggest terrestrially derived OM, as has been  
519 observed in other environments where terrestrially-derived organic molecules have a high  
520 abundance of vascular-plant derived material such as lignin (Hedges and Oades, 1997; Ward et  
521 al., 2013). These characteristics also align with reports of saturated soil environments (e.g.,  
522 floodplains) exhibiting greater abundance of less-oxygenated organic matter than aerobic  
523 environments (e.g., upland soils) as reported by Tfaily et al., 2014 in organic matter



524 transformation of a peat column. Our observed landscape gradients in compound class  
525 composition indicate spatially structured inputs of organic C such as particulate OM deposition  
526 (Langley et al., 2007). Combining this outcome with gradients observed in the total number of  
527 biochemical transformations and the contribution of heteroatoms suggests that sources of C  
528 (marine vs terrestrial) and *in situ* processing combine to influence landscape-scale gradients  
529 molecular-level organic C chemistry.

530

#### 531 **4.4 Ecological assembly processes are weakly associated with organic C**

532 Our results show that microbial community assembly is driven by a combination of dispersal  
533 limitation (a stochastic process) and deterministic selection most likely associated with pH, as is  
534 often observed in soils (Fierer, 2017; Fierer and Jackson, 2006; Garbeva et al., 2004). In contrast,  
535 variation in organic C character was associated primarily with specific conductivity. This  
536 suggests that the composition of microbial communities is not mechanistically related to C  
537 chemistry. Consistent with this inference, we found a very weak association between  $\beta$ NTI and  
538 organic C characteristics. Furthermore, and contrary to our hypothesis, we observed a weak  
539 negative association between the influence of deterministic processes and the number of organic  
540 C transformations.

541

542 Relatively fast dynamics of organic C compounds compared to relatively slow changes in  
543 microbial composition may underlie the lack of association between assembly processes and C  
544 chemistry (Bramucci et al., 2013). Supporting this interpretation, a recent study evaluating  
545 microbial community composition and C biogeochemistry of soils in a mesohaline marsh  
546 following saltwater intrusion reported immediate changes in C mineralization rates with delayed  
547 shifts in microbial community composition (Dang et al., 2019). Similarly, a 17-year dryland soil



548 transplant experiment showed large shifts in microbial activity with no change in community  
549 composition (Bond-Lamberty et al., 2016). Furthermore, studies across diverse systems show  
550 disconnect in function and composition. For example, C chemistry and not microbial community  
551 structure or gene expression was found to significantly influence freshwater hyporheic zone  
552 organic matter processing (Graham et al., 2018); environmental conditions influenced the  
553 distribution of functional groups, but not taxonomic composition of marine bacterial and  
554 archaeal communities (Lima-Mendez et al., 2015; Louca et al., 2016); and dynamic community  
555 shifts did not impact functional stability of a methanogenic reactor (Fernández et al., 1999).  
556 Combining our study with these previous investigations provides evidence that soil microbial  
557 community composition does not strongly influence biogeochemical function.

558

559 In our system, lack of an association between microbial composition and organic C chemistry is  
560 also likely due to a strong influence of stochastic community assembly. Our null modeling  
561 indicated that dispersal limitation was responsible for 54% of variation in community  
562 composition. Dispersal limitation influences composition by restricting the movement of  
563 organisms through space. Restricted movement enhances the influences of stochastic ecological  
564 drift, which arises through birth and death events that are randomly distributed across taxa  
565 (Green et al., 2004, 2008; Hubbell, 2001; Martiny et al., 2006; McClain et al., 2012; Stegen et  
566 al., 2015). This can result in functionally redundant taxa across the landscape (Loreau, 2004).  
567 Moreover, one can argue as per Louca et al., 2018 that in an open system with regular exposure  
568 to external inputs (e.g., via tides), functional redundancy is expected to occur and lead to a  
569 decoupling of microbial structure and function (Burke et al., 2011; Liebold and Chase, 2017;  
570 Nemergut et al., 2013b).

571



572 **Conclusions**

573 Our results have revealed landscape scale gradients in soil C chemistry in a coastal forested  
574 floodplain, but also show that such gradients are different across soil depths and OC fractions—  
575 occurring only in the shallow, water soluble C pool. In addition, we found little evidence of an  
576 association between C chemistry and microbial community assembly processes, likely due to a  
577 dominant influence of stochastic community assembly (as indicated by a strong influence of  
578 dispersal limitation). We propose that the disconnect between C chemistry and microbial  
579 communities is enhanced by differences in the time scales for which C chemistry and microbial  
580 community composition shift.

581

582 Our findings suggest that cross-system heterogeneity observed in coastal soil biogeochemical  
583 responses to salinity are likely associated with molecular-level C chemistry and microbial  
584 physiological responses that are contingent on historical conditions (Goldman et al., 2017;  
585 Hawkes and Keitt, 2015; Hawkes et al., 2017; Stegen et al., 2018a). We further suggest that  
586 microbial community composition may not strongly influence biogeochemical function in  
587 coastal soils. Processes associated with molecular-level C chemistry dynamics are therefore  
588 likely to be a critical component of ecosystem responses to changing salinity dynamics in coastal  
589 TAIs. A full elucidation of these processes will lay a foundation for the development of  
590 mechanistic models of coastal TAI biogeochemical dynamics, providing an opportunity for  
591 better representation of these ecosystems in local, regional, and Earth system models.

592

593 **Code and data availability**

594 Raw sequence data has been uploaded to the National Center for Biotechnology Information's  
595 (NCBI) Sequence Read Archive (SRA) under BioProject PRJNA541992. All other data files and



596 codes will be uploaded to the Department of Energy's (DOE) Environmental Systems Science  
597 Data Infrastructure for a Virtual Ecosystem (ESS-DIVE) upon manuscript acceptance. Original  
598 codes for community assembly metric calculation are available at Stegen\_etal\_ISME 2013  
599 github repository [https://github.com/stegen/Stegen\\_etal\\_ISME\\_2013](https://github.com/stegen/Stegen_etal_ISME_2013).

600

#### 601 **Author contribution**

602 AS designed the study, performed the experiments, conducted data analyses and interpretation,  
603 and wrote the original draft. JI and CG collected the samples and created site maps. MTF, RKC,  
604 and JT provided input on FTICR methodology, conducted the FTICR-MS instrument run, and  
605 handled quality filtering and pre-processing of FTICR scans. VLB and NDW contributed to  
606 funding acquisition, site selection, study design conceptualization, interpretation of results and  
607 editing. JCS contributed to funding acquisition, study design conceptualization, interpretation of  
608 results, reviewing and editing. All authors provided feedback on the manuscript.

609

#### 610 **Competing interests**

611 The authors declare no conflict of interest.

612

#### 613 **Acknowledgements**

614 This work is part of the PREMIS Initiative at Pacific Northwest National Laboratory (PNNL). It  
615 was conducted under the Laboratory Directed Research and Development Program at PNNL, a  
616 multi-program national laboratory operated by Battelle for the U.S. Department of Energy under



617 Contract DE-AC05-76RL01830. A portion of the research was performed using EMSL  
618 (grid.436923.9), a DOE Office of Science User Facility sponsored by the Office of Biological  
619 and Environmental Research. We would like to acknowledge Yuliya Farris and Sarah Fansler for  
620 DNA extraction and sequencing respectively, Colin Brislawn for processing amplicon-sequence  
621 data, and the Central Analytical Laboratory at Oregon State University for conducting soil  
622 chemical analysis.

623

#### 624 **References**

- 625 Ardón, M., Helton, A. M. and Bernhardt, E. S.: Drought and saltwater incursion synergistically  
626 reduce dissolved organic carbon export from coastal freshwater wetlands, *Biogeochemistry*,  
627 127(2–3), 411–426, doi:10.1007/s10533-016-0189-5, 2016.
- 628 Ardón, M., Helton, A. M. and Bernhardt, E. S.: Salinity effects on greenhouse gas emissions  
629 from wetland soils are contingent upon hydrologic setting: a microcosm experiment,  
630 *Biogeochemistry*, 140(2), 217–232, doi:10.1007/s10533-018-0486-2, 2018.
- 631 Bailey, V. L., Smith, A. P., Tfaily, M., Fansler, S. J. and Bond-Lamberty, B.: Differences in  
632 soluble organic carbon chemistry in pore waters sampled from different pore size domains, *Soil*  
633 *Biol. Biochem.*, 107, 133–143, doi:10.1016/J.SOILBIO.2016.11.025, 2017.
- 634 Barry, S. C., Bianchi, T. S., Shields, M. R., Hutchings, J. A., Jacoby, C. A. and Frazer, T. K.:  
635 Characterizing blue carbon stocks in *Thalassia testudinum* meadows subjected to different  
636 phosphorus supplies: A lignin biomarker approach, *Limnol. Oceanogr.*, doi:10.1002/lno.10965,  
637 2018.
- 638 Bischoff, N., Mikutta, R., Shibistova, O., Dohrmann, R., Herdtle, D., Gerhard, L., Fritzsche, F.,  
639 Puzanov, A., Silanteva, M., Grebennikova, A. and Guggenberger, G.: Organic matter dynamics  
640 along a salinity gradient in Siberian steppe soils, *Biogeosciences*, 15, 13–29, doi:10.5194/bg-15-  
641 13-2018, 2018.
- 642 Bond-Lamberty, B., Bolton, H., Fansler, S., Heredia-Langner, A., Liu, C., McCue, L. A., Smith,  
643 J. and Bailey, V.: Soil Respiration and Bacterial Structure and Function after 17 Years of a  
644 Reciprocal Soil Transplant Experiment, edited by K. Treseder, *PLoS One*, 11(3), e0150599,  
645 doi:10.1371/journal.pone.0150599, 2016.
- 646 Bottos, E. M., Kennedy, D. W., Romero, E. B., Fansler, S. J., Brown, J. M., Bramer, L. M., Chu,  
647 R. K., Tfaily, M. M., Jansson, J. K. and Stegen, J. C.: Dispersal limitation and thermodynamic  
648 constraints govern spatial structure of permafrost microbial communities, *FEMS Microbiol.*  
649 *Ecol.*, 94(8), doi:10.1093/femsec/fiy110, 2018.
- 650 Boye, K., Noël, V., Tfaily, M. M., Bone, S. E., Williams, K. H., Bargar, J. R. and Fendorf, S.:



- 651 Thermodynamically controlled preservation of organic carbon in floodplains, ,  
652 doi:10.1038/NGEO2940, 2017.
- 653 Bramucci, A., Han, S., Beckers, J., Haas, C., Lanoil, B., Bramucci, A., Han, S., Beckers, J.,  
654 Haas, C. and Lanoil, B.: Composition, Diversity, and Stability of Microbial Assemblages in  
655 Seasonal Lake Ice, Miquelon Lake, Central Alberta, *Biology (Basel)*., 2(2), 514–532,  
656 doi:10.3390/biology2020514, 2013.
- 657 Breitling, R., Ritchie, S., Goodenowe, D., Stewart, M. L. and Barrett, M. P.: Ab initio prediction  
658 of metabolic networks using Fourier transform mass spectrometry data, *Metabolomics*, 2(3),  
659 155–164, doi:10.1007/s11306-006-0029-z, 2006.
- 660 Brown, J., Zavoshy, N., Brislawn, C. J. and McCue, L. A.: Hundo: a Snakemake workflow for  
661 microbial community sequence data, , doi:10.7287/peerj.preprints.27272v1, 2018.
- 662 Burke, C., Steinberg, P., Rusch, D., Kjelleberg, S. and Thomas, T.: Bacterial community  
663 assembly based on functional genes rather than species., *Proc. Natl. Acad. Sci. U. S. A.*, 108(34),  
664 14288–93, doi:10.1073/pnas.1101591108, 2011.
- 665 Caruso, T., Chan, Y., Lacap, D. C., Lau, M. C. Y., McKay, C. P. and Pointing, S. B.: Stochastic  
666 and deterministic processes interact in the assembly of desert microbial communities on a global  
667 scale., *ISME J.*, 5(9), 1406–13, doi:10.1038/ismej.2011.21, 2011.
- 668 Chambers, L. G., Reddy, K. R. and Osborne, T. Z.: Short-Term Response of Carbon Cycling to  
669 Salinity Pulses in a Freshwater Wetland, *Soil Sci. Soc. Am. J.*, 75(5), 2000,  
670 doi:10.2136/sssaj2011.0026, 2011.
- 671 Chambers, L. G., Osborne, T. Z. and Reddy, K. R.: Effect of salinity-altering pulsing events on  
672 soil organic carbon loss along an intertidal wetland gradient: a laboratory experiment,  
673 *Biogeochemistry*, 115(1–3), 363–383, doi:10.1007/s10533-013-9841-5, 2013.
- 674 Chambers, L. G., Davis, S. E., Troxler, T., Boyer, J. N., Downey-Wall, A. and Scinto, L. J.:  
675 Biogeochemical effects of simulated sea level rise on carbon loss in an Everglades mangrove  
676 peat soil, *Hydrobiologia*, 726(1), 195–211, doi:10.1007/s10750-013-1764-6, 2014.
- 677 Conant, R. T., Ogle, S. M., Paul, E. A. and Paustian, K.: Measuring and monitoring soil organic  
678 carbon stocks in agricultural lands for climate mitigation, *Front. Ecol. Environ.*, 9(3), 169–173,  
679 doi:10.1890/090153, 2011.
- 680 Conrads, P. A. and Darby, L. S.: Development of a coastal drought index using salinity data,  
681 *Bull. Am. Meteorol. Soc.*, 98(4), 753–766, doi:10.1175/BAMS-D-15-00171.1, 2017.
- 682 Dang, C., Morrissey, E. M., Neubauer, S. C. and Franklin, R. B.: Novel microbial community  
683 composition and carbon biogeochemistry emerge over time following saltwater intrusion in  
684 wetlands, *Glob. Chang. Biol.*, (September 2018), 549–561, doi:10.1111/gcb.14486, 2019.
- 685 Dini-Andreote, F., Stegen, J. C., van Elsas, J. D. and Salles, J. F.: Disentangling mechanisms that  
686 mediate the balance between stochastic and deterministic processes in microbial succession.,  
687 *Proc. Natl. Acad. Sci. U. S. A.*, 112(11), E1326–32, doi:10.1073/pnas.1414261112, 2015.
- 688 Dittmar, T., Koch, B., Hertkorn, N. and Kattner, G.: A simple and efficient method for the solid-  
689 phase extraction of dissolved organic matter (SPE-DOM) from seawater, *Limnol. Ocean.*,  
690 *Methods* 6, 230–235 [online] Available from:



- 691 <https://aslopubs.onlinelibrary.wiley.com/doi/pdf/10.4319/lom.2008.6.230> (Accessed 16 April  
692 2019), 2008.
- 693 Dungait, J. A. J., Hopkins, D. W., Gregory, A. S. and Whitmore, A. P.: Soil organic matter  
694 turnover is governed by accessibility not recalcitrance, *Glob. Chang. Biol.*, 18(6), 1781–1796,  
695 doi:10.1111/j.1365-2486.2012.02665.x, 2012.
- 696 Ensign, S. H. and Noe, G. B.: Tidal extension and sea-level rise: recommendations for a research  
697 agenda, *Front. Ecol. Environ.*, 16(1), 37–43, doi:10.1002/fee.1745, 2018.
- 698 Fernández, A., Huang, S., Seston, S., Xing, J., Hickey, R., Criddle, C. and Tiedje, J.: How stable  
699 is stable? Function versus community composition., *Appl. Environ. Microbiol.*, 65(8), 3697–704  
700 [online] Available from: <http://www.ncbi.nlm.nih.gov/pubmed/10427068> (Accessed 27 March  
701 2019), 1999.
- 702 Fierer, N.: Embracing the unknown: disentangling the complexities of the soil microbiome, *Nat.*  
703 *Publ. Gr.*, doi:10.1038/nrmicro.2017.87, 2017.
- 704 Fierer, N. and Jackson, R. B.: The diversity and biogeography of soil bacterial communities.  
705 [online] Available from: [www.pnas.org/cgi/doi/10.1073/pnas.0507535103](http://www.pnas.org/cgi/doi/10.1073/pnas.0507535103) (Accessed 8 February  
706 2019), 2006.
- 707 Garbeva, P., van Veen, J. a and van Elsas, J. D.: Microbial diversity in soil: selection microbial  
708 populations by plant and soil type and implications for disease suppressiveness., *Annu. Rev.*  
709 *Phytopathol.*, 42(29), 243–70, doi:10.1146/annurev.phyto.42.012604.135455, 2004.
- 710 Goldman, A. E., Graham, E. B., Crump, A. R., Kennedy, D. W., Romero, E. B., Anderson, C.  
711 G., Dana, K. L., Resch, C. T., Fredrickson, J. K. and Stegen, J. C.: Biogeochemical cycling at the  
712 aquatic–terrestrial interface is linked to parafluvial hyporheic zone inundation history,  
713 *Biogeosciences*, 14(18), 4229–4241, doi:10.5194/bg-14-4229-2017, 2017.
- 714 Gouffi, K., Pica, N., Pichereau, V. and Blanco, C.: Disaccharides as a new class of  
715 nonaccumulated osmoprotectants for *Sinorhizobium meliloti*., *Appl. Environ. Microbiol.*, 65(4),  
716 1491–500 [online] Available from: <http://www.ncbi.nlm.nih.gov/pubmed/10103242> (Accessed 8  
717 October 2018), 1999.
- 718 Graham, C. H. and Fine, P. V. A.: Phylogenetic beta diversity: linking ecological and  
719 evolutionary processes across space in time, *Ecol. Lett.*, 11(12), 1265–1277, doi:10.1111/j.1461-  
720 0248.2008.01256.x, 2008.
- 721 Graham, E. B., Knelman, J. E., Schindlbacher, A., Siciliano, S., Breulmann, M., Yannarell, A.,  
722 Beman, J. M., Abell, G., Philippot, L., Prosser, J., Foulquier, A., Yuste, J. C., Glanville, H. C.,  
723 Jones, D. L., Angel, R., Salminen, J., Newton, R. J., Bürgmann, H., Ingram, L. J., Hamer, U.,  
724 Siljanen, H. M. P., Peltoniemi, K., Potthast, K., Bañeras, L., Hartmann, M., Banerjee, S., Yu, R.-  
725 Q., Nogaro, G., Richter, A., Koranda, M., Castle, S. C., Goberna, M., Song, B., Chatterjee, A.,  
726 Nunes, O. C., Lopes, A. R., Cao, Y., Kaisermann, A., Hallin, S., Strickland, M. S., Garcia-  
727 Pausas, J., Barba, J., Kang, H., Isobe, K., Papaspyrou, S., Pastorelli, R., Lagomarsino, A.,  
728 Lindström, E. S., Basiliko, N. and Nemergut, D. R.: Microbes as Engines of Ecosystem  
729 Function: When Does Community Structure Enhance Predictions of Ecosystem Processes?,  
730 *Front. Microbiol.*, 7, 214, doi:10.3389/fmicb.2016.00214, 2016.
- 731 Graham, E. B., Tfaily, M. M., Crump, A. R., Goldman, A. E., Bramer, L. M., Arntzen, E.,



- 732 Romero, E., Resch, C. T., Kennedy, D. W. and Stegen, J. C.: Carbon Inputs From Riparian  
733 Vegetation Limit Oxidation of Physically Bound Organic Carbon Via Biochemical and  
734 Thermodynamic Processes, *J. Geophys. Res. Biogeosciences*, 122(12), 3188–3205,  
735 doi:10.1002/2017JG003967, 2017a.
- 736 Graham, E. B., Crump, A. R., Resch, C. T., Fansler, S., Arntzen, E., Kennedy, D. W.,  
737 Fredrickson, J. K. and Stegen, J. C.: Deterministic influences exceed dispersal effects on  
738 hydrologically-connected microbiomes, *Environ. Microbiol.*, 19(4), 1552–1567,  
739 doi:10.1111/1462-2920.13720, 2017b.
- 740 Graham, E. B., Crump, A. R., Kennedy, D. W., Arntzen, E., Fansler, S., Purvine, S. O., Nicora,  
741 C. D., Nelson, W., Tfaily, M. M. and Stegen, J. C.: Multi 'omics comparison reveals  
742 metabolome biochemistry, not microbiome composition or gene expression, corresponds to  
743 elevated biogeochemical function in the hyporheic zone, *Sci. Total Environ.*, 642, 742–753,  
744 doi:10.1016/J.SCITOTENV.2018.05.256, 2018.
- 745 Green, J. L., Holmes, A. J., Westoby, M., Oliver, I., Briscoe, D., Dangerfield, M., Gillings, M.  
746 and Beattie, A. J.: Spatial scaling of microbial eukaryote diversity, *Nature*, 432(7018), 747–750,  
747 doi:10.1038/nature03034, 2004.
- 748 Green, J. L., Bohannan, B. J. M. and Whitaker, R. J.: Microbial Biogeography: From Taxonomy  
749 to Traits, *Science* (80-. ), 320(5879), 1039–1043, doi:10.1126/SCIENCE.1153475, 2008.
- 750 Guillemette, R., Kaneko, R., Blanton, J., Tan, J., Witt, M., Hamilton, S., Allen, E. E., Medina,  
751 M., Hamasaki, K., Koch, B. P. and Azam, F.: Bacterioplankton drawdown of coral mass-  
752 spawned organic matter, *ISME J.*, 12(9), 2238–2251, doi:10.1038/s41396-018-0197-7, 2018.
- 753 Hawkes, C. V. and Keitt, T. H.: Resilience vs. historical contingency in microbial responses to  
754 environmental change, edited by A. Classen, *Ecol. Lett.*, 18(7), 612–625, doi:10.1111/ele.12451,  
755 2015.
- 756 Hawkes, C. V., Waring, B. G., Rocca, J. D. and Kivlin, S. N.: Historical climate controls soil  
757 respiration responses to current soil moisture., *Proc. Natl. Acad. Sci. U. S. A.*, 114(24), 6322–  
758 6327, doi:10.1073/pnas.1620811114, 2017.
- 759 Hedges, J. I. and Oades, J. M.: Comparative organic geochemistries of soils and marine  
760 sediments, *Org. Geochem.*, 27(7/8), 319–361 [online] Available from:  
761 [http://www.riversystems.washington.edu/lc/RIVERS/93\\_hedges\\_ji\\_27-319-361.pdf](http://www.riversystems.washington.edu/lc/RIVERS/93_hedges_ji_27-319-361.pdf) (Accessed 7  
762 May 2019), 1997.
- 763 Hedges, J. I., Keil, R. G. and Benner, R.: What happens to terrestrial organic matter in the  
764 ocean?, *Org. Geochem.*, 27(5–6), 195–212, doi:10.1016/S0146-6380(97)00066-1, 1997.
- 765 Herbert, E. R., Schubauer-Berigan, J. and Craft, C. B.: Differential effects of chronic and acute  
766 simulated seawater intrusion on tidal freshwater marsh carbon cycling, *Biogeochemistry*, 138(2),  
767 137–154, doi:10.1007/s10533-018-0436-z, 2018.
- 768 Hinson, A. L., Feagin, R. A., Eriksson, M., Najjar, R. G., Herrmann, M., Bianchi, T. S., Kemp,  
769 M., Hutchings, J. A., Crooks, S. and Boutton, T.: The spatial distribution of soil organic carbon  
770 in tidal wetland soils of the continental United States, *Glob. Chang. Biol.*, 23(12), 5468–5480,  
771 doi:10.1111/gcb.13811, 2017.



- 772 Hoitink, A. J. F. and Jay, D. A.: Tidal river dynamics: Implications for deltas, *Rev. Geophys.*,  
773 54(1), 240–272, doi:10.1002/2015RG000507, 2016.
- 774 Hoitink, A. J. F., Buschman, F. A. and Vermeulen, B.: Continuous measurements of discharge  
775 from a horizontal acoustic Doppler current profiler in a tidal river, *Water Resour. Res.*, 45, 11406,  
776 doi:10.1029/2009WR007791, 2009.
- 777 Holmquist, J. R., Windham-Myers, L., Bliss, N., Crooks, S., Morris, J. T., Megonigal, J. P.,  
778 Troxler, T., Weller, D., Callaway, J., Drexler, J., Ferner, M. C., Gonneea, M. E., Kroeger, K. D.,  
779 Schile-Beers, L., Woo, I., Buffington, K., Breithaupt, J., Boyd, B. M., Brown, L. N., Dix, N.,  
780 Hice, L., Horton, B. P., MacDonald, G. M., Moyer, R. P., Reay, W., Shaw, T., Smith, E., Smoak,  
781 J. M., Sommerfield, C., Thorne, K., Velinsky, D., Watson, E., Grimes, K. W. and Woodrey, M.:  
782 Accuracy and Precision of Tidal Wetland Soil Carbon Mapping in the Conterminous United  
783 States, *Sci. Rep.*, 8(1), 9478, doi:10.1038/s41598-018-26948-7, 2018.
- 784 Hubbell, S. P.: *The Unified Neutral Theory of Biodiversity and Biogeography*, Princeton  
785 University Press. [online] Available from: <http://www.jstor.org/stable/j.ctt7rj8w>, 2001.
- 786 Jobbágy, E. G. and Jackson, R. B.: The vertical distribution of soil organic carbon and its relation  
787 to climate and vegetation, *Ecol. Appl.*, 10(2), 423–436, doi:10.1890/1051-  
788 0761(2000)010[0423:TVDOSO]2.0.CO;2, 2000.
- 789 Kim, S., Kramer, R. W. and Hatcher, P. G.: Graphical Method for Analysis of Ultrahigh-  
790 Resolution Broadband Mass Spectra of Natural Organic Matter, the Van Krevelen Diagram,  
791 *Anal. Chem.*, 75(20), 5336–5344, doi:10.1021/ac034415p, 2003.
- 792 Koch, B. P. and Dittmar, T.: From mass to structure: an aromaticity index for high-resolution  
793 mass data of natural organic matter, *Rapid Commun. Mass Spectrom.*, 20(5), 926–932,  
794 doi:10.1002/rcm.2386, 2006.
- 795 Koch, B. P. and Dittmar, T.: From mass to structure: an aromaticity index for high-resolution  
796 mass data of natural organic matter, *Rapid Commun. Mass Spectrom.*, 30(1), 250–250,  
797 doi:10.1002/rcm.7433, 2016.
- 798 Koch, B. P., Kattner, G., Witt, M. and Passow, U.: Molecular insights into the microbial  
799 formation of marine dissolved organic matter: recalcitrant or labile?, *Biogeosciences*, 11(15),  
800 4173–4190, doi:10.5194/bg-11-4173-2014, 2014.
- 801 Kramer, C. and Gleixner, G.: Variable use of plant- and soil-derived carbon by microorganisms  
802 in agricultural soils, *Soil Biol. Biochem.*, 38(11), 3267–3278,  
803 doi:10.1016/J.SOILBIO.2006.04.006, 2006.
- 804 Kramer, C. and Gleixner, G.: Soil organic matter in soil depth profiles: Distinct carbon  
805 preferences of microbial groups during carbon transformation, *Soil Biol. Biochem.*, 40(2), 425–  
806 433, doi:10.1016/J.SOILBIO.2007.09.016, 2008.
- 807 Krauss, K. W., Noe, G. B., Duberstein, J. A., Conner, W. H., Stagg, C. L., Cormier, N., Jones,  
808 M. C., Bernhardt, C. E., Graeme Lockaby, B., From, A. S., Doyle, T. W., Day, R. H., Ensign, S.  
809 H., Pierfelice, K. N., Hupp, C. R., Chow, A. T. and Whitbeck, J. L.: The Role of the Upper Tidal  
810 Estuary in Wetland Blue Carbon Storage and Flux, *Global Biogeochem. Cycles*, 32(5), 817–839,  
811 doi:10.1029/2018GB005897, 2018.



- 812 Ksionzek, K. B., Lechtenfeld, O. J., McCallister, S. L., Schmitt-Kopplin, P., Geuer, J. K.,  
813 Geibert, W. and Koch, B. P.: Dissolved organic sulfur in the ocean: Biogeochemistry of a  
814 petagram inventory., *Science*, 354(6311), 456–459, doi:10.1126/science.aaf7796, 2016.
- 815 Kubartová, A., Ottosson, E. and Stenlid, J.: Linking fungal communities to wood density loss  
816 after 12 years of log decay, *FEMS Microbiol. Ecol.*, 91(5), doi:10.1093/femsec/fiv032, 2015.
- 817 Kujawinski, E. B. and Behn, M. D.: Automated analysis of electrospray ionization fourier  
818 transform ion cyclotron resonance mass spectra of natural organic matter., *Anal. Chem.*, 78(13),  
819 4363–73, doi:10.1021/ac0600306, 2006.
- 820 Langer, U. and Rinklebe, J.: Lipid biomarkers for assessment of microbial communities in  
821 floodplain soils of the Elbe River (Germany), *Wetlands*, 29(1), 353–362, doi:10.1672/08-114.1,  
822 2009.
- 823 Langley, J. A., Sigrist, M. V, Duls, J., Cahoon, D. R., Lynch, J. C. and Megonigal, J. P.: Global  
824 Change and Marsh Elevation Dynamics: Experimenting Where Land Meets Sea and Biology  
825 Meets Geology, in *Proceedings of the Smithsonian Marine Sciences Symposium*, pp. 391–400,  
826 Smithsonian Institution Scholarly Press, , Washington, DC. [online] Available from:  
827 [https://repository.si.edu/bitstream/handle/10088/18988/serc\\_Langley\\_et\\_al.\\_2009\\_Smithsonian\\_](https://repository.si.edu/bitstream/handle/10088/18988/serc_Langley_et_al._2009_Smithsonian_Marine_Sciences_.pdf?sequence=1&isAllowed=y)  
828 [Marine\\_Sciences\\_.pdf?sequence=1&isAllowed=y](https://repository.si.edu/bitstream/handle/10088/18988/serc_Langley_et_al._2009_Smithsonian_Marine_Sciences_.pdf?sequence=1&isAllowed=y) (Accessed 7 May 2019), 2007.
- 829 Langston, A. K., Kaplan, D. A. and Putz, F. E.: A casualty of climate change? Loss of freshwater  
830 forest islands on Florida’s Gulf Coast, *Glob. Chang. Biol.*, 23(12), 5383–5397,  
831 doi:10.1111/gcb.13805, 2017.
- 832 LaRowe, D. E. and Van Cappellen, P.: Degradation of natural organic matter: A thermodynamic  
833 analysis, *Geochim. Cosmochim. Acta*, 75(8), 2030–2042, doi:10.1016/J.GCA.2011.01.020,  
834 2011.
- 835 Lechtenfeld, O. J., Hertkorn, N., Shen, Y., Witt, M. and Benner, R.: Marine sequestration of  
836 carbon in bacterial metabolites., *Nat. Commun.*, 6(1), 6711, doi:10.1038/ncomms7711, 2015.
- 837 Liebold, M. A. and Chase, M. J.: Combining Taxonomic and Functional Patterns to Disentangle  
838 Metacommunity Assembly Processes, in *Metacommunity Ecology*, Volume 9, edited by M. A.  
839 Liebold and M. J. Chase, p. 504, Princeton University Press, Princeton, New Jersey., 2017.
- 840 Lima-Mendez, G., Faust, K., Henry, N., Decelle, J., Colin, S., Carcillo, F., Chaffron, S., Ignacio-  
841 Espinosa, J. C., Roux, S., Vincent, F., Bittner, L., Darzi, Y., Wang, J., Audic, S., Berline, L.,  
842 Bontempi, G., Cabello, A. M., Coppola, L., Cornejo-Castillo, F. M., d’Ovidio, F., Meester, L.  
843 De, Ferrera, I., Garet-Delmas, M.-J., Guidi, L., Lara, E., Pesant, S., Royo-Llonch, M., Salazar,  
844 G., Sánchez, P., Sebastian, M., Souffreau, C., Dimier, C., Picheral, M., Searson, S., Kandels-  
845 Lewis, S., coordinators, T. O., Gorsky, G., Not, F., Ogata, H., Speich, S., Stemmann, L.,  
846 Weissenbach, J., Wincker, P., Acinas, S. G., Sunagawa, S., Bork, P., Sullivan, M. B., Karsenti,  
847 E., Bowler, C., Vargas, C. de and Raes, J.: Determinants of community structure in the global  
848 plankton interactome, *Science* (80-. ), 348(6237), 1262073, doi:10.1126/SCIENCE.1262073,  
849 2015.
- 850 Liu, X., Ruecker, A., Song, B., Xing, J., Conner, W. H. and Chow, A. T.: Effects of salinity and  
851 wet–dry treatments on C and N dynamics in coastal-forested wetland soils: Implications of sea  
852 level rise, *Soil Biol. Biochem.*, 112, 56–67, doi:10.1016/J.SOILBIO.2017.04.002, 2017.



- 853 Loreau, M.: Does functional redundancy exist?, *Oikos*, 104(3), 606–611, doi:10.1111/j.0030-  
854 1299.2004.12685.x, 2004.
- 855 Louca, S., Parfrey, L. W. and Doebeli, M.: Decoupling function and taxonomy in the global  
856 ocean microbiome., *Science*, 353(6305), 1272–7, doi:10.1126/science.aaf4507, 2016.
- 857 Louca, S., Polz, M. F., Mazel, F., Albright, M. B. N., Huber, J. A., O’connor, M. I., Ackermann,  
858 M., Hahn, A. S., Srivastava, D. S., Crowe, S. A., Doebeli, M. and Parfrey, L. W.: Disentangling  
859 function from taxonomy in microbial systems Function and functional redundancy in microbial  
860 systems, , doi:10.1038/s41559-018-0519-1, 2018.
- 861 Martiny, J. B. H., Bohannan, B. J. M., Brown, J. H., Colwell, R. K., Fuhrman, J. A., Green, J. L.,  
862 Horner-Devine, M. C., Kane, M., Krumins, J. A., Kuske, C. R., Morin, P. J., Naeem, S., Øvreås,  
863 L., Reysenbach, A.-L., Smith, V. H. and Staley, J. T.: Microbial biogeography: putting  
864 microorganisms on the map, *Nat. Rev. Microbiol.*, 4(2), 102–112, doi:10.1038/nrmicro1341,  
865 2006.
- 866 Marton, J. M., Herbert, E. R. and Craft, C. B.: Effects of Salinity on Denitrification and  
867 Greenhouse Gas Production from Laboratory-incubated Tidal Forest Soils, *Wetlands*, 32(2),  
868 347–357, doi:10.1007/s13157-012-0270-3, 2012.
- 869 Mau, R. L., Liu, C. M., Aziz, M., Schwartz, E., Dijkstra, P., Marks, J. C., Price, L. B., Keim, P.  
870 and Hungate, B. A.: Linking soil bacterial biodiversity and soil carbon stability, *ISME J.*, 9(6),  
871 1477–1480, doi:10.1038/ismej.2014.205, 2015.
- 872 McCarthy, M., Dimmitt, B., Muller-Karger, F., McCarthy, M. J., Dimmitt, B. and Muller-  
873 Karger, F. E.: Rapid Coastal Forest Decline in Florida’s Big Bend, *Remote Sens.*, 10(11), 1721,  
874 doi:10.3390/rs10111721, 2018.
- 875 McClain, C. R., Stegen, J. C. and Hurlbert, A. H.: Dispersal, environmental niches and oceanic-  
876 scale turnover in deep-sea bivalves, *Proc. R. Soc. B Biol. Sci.*, doi:10.1098/RSPB.2011.2166,  
877 2012.
- 878 Medeiros, P. M., Seidel, M., Ward, N. D., Carpenter, E. J., Gomes, H. R., Niggemann, J.,  
879 Krusche, A. V., Richey, J. E., Yager, P. L. and Dittmar, T.: Fate of the Amazon River dissolved  
880 organic matter in the tropical Atlantic Ocean, *Global Biogeochem. Cycles*, 29(5), 677–690,  
881 doi:10.1002/2015GB005115, 2015.
- 882 Minor, E. C., Steinbring, C. J., Longnecker, K. and Kujawinski, E. B.: Characterization of  
883 dissolved organic matter in Lake Superior and its watershed using ultrahigh resolution mass  
884 spectrometry, *Org. Geochem.*, 43, 1–11, doi:10.1016/J.ORGGEOCHEM.2011.11.007, 2012.
- 885 Nemergut, D. R., Schmidt, S. K., Fukami, T., O’Neill, S. P., Bilinski, T. M., Stanish, L. F.,  
886 Knelman, J. E., Darcy, J. L., Lynch, R. C., Wickey, P. and Ferrenberg, S.: Patterns and processes  
887 of microbial community assembly., *Microbiol. Mol. Biol. Rev.*, 77(3), 342–56,  
888 doi:10.1128/MMBR.00051-12, 2013a.
- 889 Nemergut, D. R., Schmidt, S. K., Fukami, T., O’Neill, S. P., Bilinski, T. M., Stanish, L. F.,  
890 Knelman, J. E., Darcy, J. L., Lynch, R. C., Wickey, P. and Ferrenberg, S.: Patterns and processes  
891 of microbial community assembly., *Microbiol. Mol. Biol. Rev.*, 77(3), 342–56,  
892 doi:10.1128/MMBR.00051-12, 2013b.



- 893 Neubauer, S. C., Givler, K., Valentine, S. and Megonigal, J. P.: Seasonal patterns and plant-  
894 mediated controls of subsurface wetland biogeochemistry, *Ecology*, 86(12), 3334–3344,  
895 doi:10.1890/04-1951, 2005.
- 896 Neubauer, S. C., Franklin, R. B. and Berrier, D. J.: Saltwater intrusion into tidal freshwater  
897 marshes alters the biogeochemical processing of organic carbon, *Biogeosciences*, 10(12), 8171–  
898 8183, doi:10.5194/bg-10-8171-2013, 2013.
- 899 Nyman, J. A. and Delaune, R. D.: CO<sub>2</sub> emission and soil Eh responses to different hydrological  
900 conditions in fresh, brackish, and saline marsh soils. [online] Available from:  
901 <https://aslopubs.onlinelibrary.wiley.com/doi/pdf/10.4319/lo.1991.36.7.1406> (Accessed 31  
902 October 2018), 1991.
- 903 R Development Core Team: The R Project for Statistical Computing. [online] Available from:  
904 <https://www.r-project.org/> (Accessed 9 May 2019), 2019.
- 905 Reynolds, L. L., Lajtha, K., Bowden, R. D., Tfaily, M. M., Johnson, B. R. and Bridgham, S. D.:  
906 The Path From Litter to Soil: Insights Into Soil C Cycling From Long-Term Input Manipulation  
907 and High-Resolution Mass Spectrometry, *J. Geophys. Res. Biogeosciences*, 123(5), 1486–1497,  
908 doi:10.1002/2017JG004076, 2018.
- 909 Rivas-Ubach, A., Liu, Y., Bianchi, T. S., Tolić, N., Jansson, C. and Paša-Tolić, L.: Moving  
910 beyond the van Krevelen Diagram: A New Stoichiometric Approach for Compound  
911 Classification in Organisms, *Anal. Chem.*, 90(10), 6152–6160,  
912 doi:10.1021/acs.analchem.8b00529, 2018.
- 913 Roberts, M. F.: Organic compatible solutes of halotolerant and halophilic microorganisms.,  
914 *Saline Systems*, 1, 5, doi:10.1186/1746-1448-1-5, 2005.
- 915 Rocca, J. D., Hall, E. K., Lennon, J. T., Evans, S. E., Waldrop, M. P., Cotner, J. B., Nemergut,  
916 D. R., Graham, E. B. and Wallenstein, M. D.: Relationships between protein-encoding gene  
917 abundance and corresponding process are commonly assumed yet rarely observed, *ISME J.*, 9(8),  
918 1693–1699, doi:10.1038/ismej.2014.252, 2015.
- 919 Sawakuchi, H. O., Neu, V., Ward, N. D., Barros, M. de L. C., Valerio, A. M., Gagne-Maynard,  
920 W., Cunha, A. C., Less, D. F. S., Diniz, J. E. M., Brito, D. C., Krusche, A. V. and Richey, J. E.:  
921 Carbon Dioxide Emissions along the Lower Amazon River, *Front. Mar. Sci.*, 4,  
922 doi:10.3389/fmars.2017.00076, 2017.
- 923 Schmidt, M. W. I., Torn, M. S., Abiven, S., Dittmar, T., Guggenberger, G., Janssens, I. A.,  
924 Kleber, M., Kögel-Knabner, I., Lehmann, J., Manning, D. A. C., Nannipieri, P., Rasse, D. P.,  
925 Weiner, S. and Trumbore, S. E.: Persistence of soil organic matter as an ecosystem property,  
926 *Nature*, 478(7367), 49–56, doi:10.1038/nature10386, 2011.
- 927 Seidel, M., Dittmar, T., Ward, N. D., Krusche, A. V., Richey, J. E., Yager, P. L. and Medeiros,  
928 P. M.: Seasonal and spatial variability of dissolved organic matter composition in the lower  
929 Amazon River, *Biogeochemistry*, 131(3), 281–302, doi:10.1007/s10533-016-0279-4, 2016.
- 930 Shen, Y., Chapelle, F. H., Strom, E. W. and Benner, R.: Origins and bioavailability of dissolved  
931 organic matter in groundwater, *Biogeochemistry*, 122(1), 61–78, doi:10.1007/s10533-014-0029-  
932 4, 2015.



- 933 Simon, C., Roth, V.-N., Dittmar, T. and Gleixner, G.: Molecular Signals of Heterogeneous  
934 Terrestrial Environments Identified in Dissolved Organic Matter: A Comparative Analysis of  
935 Orbitrap and Ion Cyclotron Resonance Mass Spectrometers, *Front. Earth Sci.*, 6, 138,  
936 doi:10.3389/feart.2018.00138, 2018.
- 937 Sleator, R. D. and Hill, C.: Bacterial osmoadaptation: the role of osmolytes in bacterial stress and  
938 virulence., *FEMS Microbiol. Rev.*, 26(1), 49–71 [online] Available from:  
939 <http://www.ncbi.nlm.nih.gov/pubmed/12007642> (Accessed 8 October 2018), 2002.
- 940 Smith, C. J., DeLaune, R. D. and Patrick, W. H.: Carbon dioxide emission and carbon  
941 accumulation in coastal wetlands, *Estuar. Coast. Shelf Sci.*, 17(1), 21–29, doi:10.1016/0272-  
942 7714(83)90042-2, 1983.
- 943 Stegen, J. C., Lin, X., Konopka, A. E. and Fredrickson, J. K.: Stochastic and deterministic  
944 assembly processes in subsurface microbial communities., *ISME J.*, 6(9), 1653–64,  
945 doi:10.1038/ismej.2012.22, 2012.
- 946 Stegen, J. C., Lin, X., Fredrickson, J. K., Chen, X., Kennedy, D. W., Murray, C. J., Rockhold, M.  
947 L. and Konopka, A.: Quantifying community assembly processes and identifying features that  
948 impose them, *ISME J.*, 7(11), 2069–2079, doi:10.1038/ismej.2013.93, 2013.
- 949 Stegen, J. C., Lin, X., Fredrickson, J. K. and Konopka, A. E.: Estimating and mapping ecological  
950 processes influencing microbial community assembly, *Front. Microbiol.*, 6, 370,  
951 doi:10.3389/fmicb.2015.00370, 2015.
- 952 Stegen, J. C., Bottos, E. M. and Jansson, J. K.: A unified conceptual framework for prediction  
953 and control of microbiomes, *Curr. Opin. Microbiol.*, 44, 20–27, doi:10.1016/J.MIB.2018.06.002,  
954 2018a.
- 955 Stegen, J. C., Johnson, T., Fredrickson, J. K., Wilkins, M. J., Konopka, A. E., Nelson, W. C.,  
956 Arntzen, E. V., Chrisler, W. B., Chu, R. K., Fansler, S. J., Graham, E. B., Kennedy, D. W.,  
957 Resch, C. T., Tfaily, M. and Zachara, J.: Influences of organic carbon speciation on hyporheic  
958 corridor biogeochemistry and microbial ecology, *Nat. Commun.*, 9(1), 1–11,  
959 doi:10.1038/s41467-018-02922-9, 2018b.
- 960 Stegen, J. C., Johnson, T., Fredrickson, J. K., Wilkins, M. J., Konopka, A. E., Nelson, W. C.,  
961 Arntzen, E. V., Chrisler, W. B., Chu, R. K., Fansler, S. J., Graham, E. B., Kennedy, D. W.,  
962 Resch, C. T., Tfaily, M. and Zachara, J.: Influences of organic carbon speciation on hyporheic  
963 corridor biogeochemistry and microbial ecology, *Nat. Commun.*, 9(1), 585, doi:10.1038/s41467-  
964 018-02922-9, 2018c.
- 965 Steinmuller, H. E. and Chambers, L. G.: Can Saltwater Intrusion Accelerate Nutrient Export  
966 from Freshwater Wetland Soils? An Experimental Approach, *Soil Sci. Soc. Am. J.*, 82(1), 283,  
967 doi:10.2136/sssaj2017.05.0162, 2018.
- 968 Tank, S. E., Fellman, J. B., Hood, E. and Kritzberg, E. S.: Beyond respiration: Controls on lateral  
969 carbon fluxes across the terrestrial-aquatic interface, *Limnol. Oceanogr. Lett.*, 3(3), 76–88,  
970 doi:10.1002/lol2.10065, 2018.
- 971 Tfaily, M. M., Cooper, W. T., Kostka, J. E., Chanton, P. R., Schadt, C. W., Hanson, P. J.,  
972 Iversen, C. M. and Chanton, J. P.: Organic matter transformation in the peat column at Marcell  
973 Experimental Forest: Humification and vertical stratification, *JGR Biogeosciences*, (661–675),



- 974 doi:10.1002/2013JG002492, 2014.
- 975 Tfaily, M. M., Chu, R. K., Tolić, N., Roscioli, K. M., Anderton, C. R., Paša-Tolić, L., Robinson,  
976 E. W. and Hess, N. J.: Advanced Solvent Based Methods for Molecular Characterization of Soil  
977 Organic Matter by High-Resolution Mass Spectrometry, *Anal. Chem.*, 87(10), 5206–5215,  
978 doi:10.1021/acs.analchem.5b00116, 2015.
- 979 Tfaily, M. M., Chu, R. K., Toyoda, J., Tolić, N., Robinson, E. W., Paša-Tolić, L. and Hess, N. J.:  
980 Sequential extraction protocol for organic matter from soils and sediments using high resolution  
981 mass spectrometry, *Anal. Chim. Acta*, 972, 54–61, doi:10.1016/J.ACA.2017.03.031, 2017.
- 982 Tolić, N., Liu, Y., Liyu, A., Shen, Y., Tfaily, M. M., Kujawinski, E. B., Longnecker, K., Kuo,  
983 L.-J., Robinson, E. W., Paša-Tolić, L. and Hess, N. J.: Formularity: Software for Automated  
984 Formula Assignment of Natural and Other Organic Matter from Ultrahigh-Resolution Mass  
985 Spectra, *Anal. Chem.*, 89(23), 12659–12665, doi:10.1021/acs.analchem.7b03318, 2017.
- 986 Trivedi, P., Delgado-Baquerizo, M., Trivedi, C., Hu, H., Anderson, I. C., Jeffries, T. C., Zhou, J.  
987 and Singh, B. K.: Microbial regulation of the soil carbon cycle: evidence from gene–enzyme  
988 relationships, *ISME J.*, 10(11), 2593–2604, doi:10.1038/ismej.2016.65, 2016.
- 989 Tzortziou, M., Neale, P. J., Megonigal, P., Pow, C. L. and Butterworth, M.: Spatial gradients in  
990 dissolved carbon due to tidal marsh outwelling into a Chesapeake Bay estuary, *Mar. Ecol. Prog.  
991 Ser.*, 426, 41–56, doi:10.3354/meps09017, 2011.
- 992 U.S. DOE.: Research Priorities to Incorporate Terrestrial-Aquatic Interfaces in Earth System  
993 Models: Workshop Report, DOE/SC-0187, 2017.
- 994 Vidon, P., Allan, C., Burns, D., Duval, T. P., Gurwick, N., Inamdar, S., Lowrance, R., Okay, J.,  
995 Scott, D. and Sebestyen, S.: Hot Spots and Hot Moments in Riparian Zones: Potential for  
996 Improved Water Quality Management <sup>1</sup>, *JAWRA J. Am. Water Resour. Assoc.*, 46(2), 278–298,  
997 doi:10.1111/j.1752-1688.2010.00420.x, 2010.
- 998 van der Wal, A., Ottosson, E. and de Boer, W.: Neglected role of fungal community composition  
999 in explaining variation in wood decay rates, *Ecology*, 96(1), 124–133, doi:10.1890/14-0242.1,  
1000 2015.
- 1001 Ward, C. P., Nalven, S. G., Crump, B. C., Kling, G. W. and Cory, R. M.: Photochemical  
1002 alteration of organic carbon draining permafrost soils shifts microbial metabolic pathways and  
1003 stimulates respiration, , doi:10.1038/s41467-017-00759-2, 2017a.
- 1004 Ward, N. D., Keil, R. G., Medeiros, P. M., Brito, D. C., Cunha, A. C., Dittmar, T., Yager, P. L.,  
1005 Krusche, A. V. and Richey, J. E.: Degradation of terrestrially derived macromolecules in the  
1006 Amazon River, *Nat. Geosci.*, 6(7), 530–533, doi:10.1038/ngeo1817, 2013.
- 1007 Ward, N. D., Bianchi, T. S., Medeiros, P. M., Seidel, M., Richey, J. E., Keil, R. G. and  
1008 Sawakuchi, H. O.: Where Carbon Goes When Water Flows: Carbon Cycling across the Aquatic  
1009 Continuum, *Front. Mar. Sci.*, 4(January), doi:10.3389/fmars.2017.00007, 2017b.
- 1010 Ward, N. D., Indivero, J., Gunn, C., Wang, W., Bailey, V. and McDowell, N. G.: Longitudinal  
1011 gradients in tree stem greenhouse gas concentrations across six Pacific Northwest coastal forests,  
1012 *J. Geophys. Res. Biogeosciences*, 2019JG005064, doi:10.1029/2019JG005064, 2019a.
- 1013 Ward, N. D., Morrison, E. S., Liu, Y., Rivas-Ubach, A., Osborne, T. Z., Ogram, A. V. and



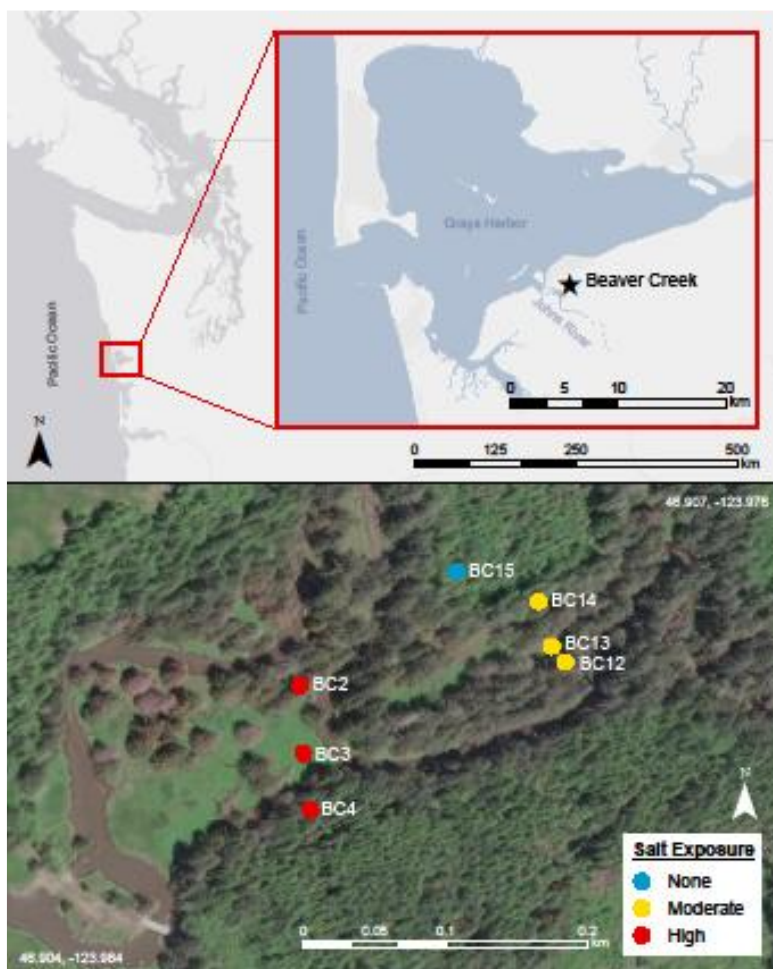
- 1014 Bianchi, T. S.: Marine microbial community responses related to wetland carbon mobilization in  
1015 the coastal zone, *Limnol. Oceanogr. Lett.*, 4(1), 25–33, doi:10.1002/lol2.10101, 2019b.
- 1016 Washington Department of Fish and Wildlife: Fish Passage & Diversion Screening  
1017 Inventory., 2019.
- 1018 Weston, N. B., Dixon, R. E. and Joye, S. B.: Ramifications of increased salinity in tidal  
1019 freshwater sediments: Geochemistry and microbial pathways of organic matter mineralization, *J.*  
1020 *Geophys. Res.*, 111(G1), G01009, doi:10.1029/2005JG000071, 2006.
- 1021 Weston, N. B., Vile, M. A., Neubauer, S. C. and Velinsky, D. J.: Accelerated microbial organic  
1022 matter mineralization following salt-water intrusion into tidal freshwater marsh soils,  
1023 *Biogeochemistry*, 102(1–3), 135–151, doi:10.1007/s10533-010-9427-4, 2011.
- 1024 Weston, N. B., Neubauer, S. C., Velinsky, D. J. and Vile, M. A.: Net ecosystem carbon exchange  
1025 and the greenhouse gas balance of tidal marshes along an estuarine salinity gradient,  
1026 *Biogeochemistry*, 120(1–3), 163–189, doi:10.1007/s10533-014-9989-7, 2014.
- 1027 Yang, J., Zhan, C., Li, Y., Zhou, D., Yu, Y. and Yu, J.: Effect of salinity on soil respiration in  
1028 relation to dissolved organic carbon and microbial characteristics of a wetland in the Liaohe  
1029 River estuary, Northeast China, *Sci. Total Environ.*, 642, 946–953,  
1030 doi:10.1016/J.SCITOTENV.2018.06.121, 2018.
- 1031 Zark, M. and Dittmar, T.: Universal molecular structures in natural dissolved organic matter.,  
1032 *Nat. Commun.*, 9(1), 3178, doi:10.1038/s41467-018-05665-9, 2018.
- 1033
- 1034
- 1035
- 1036
- 1037
- 1038
- 1039
- 1040
- 1041
- 1042
- 1043
- 1044
- 1045
- 1046
- 1047



1048 **Table 1.** Relative peak abundances (%) of compound classes in the water extracted organic  
 1049 carbon fraction averaged across replicates per site. Samples are ordered according to their depth  
 1050 profile (shallow and deep) and their relative position in the landscape: floodplain (Fp), inland (I),  
 1051 and upland (U). Abbreviations: Con HC (condensed hydrocarbon), UnsatHC (unsaturated  
 1052 hydrocarbon), Other (no classification assigned)

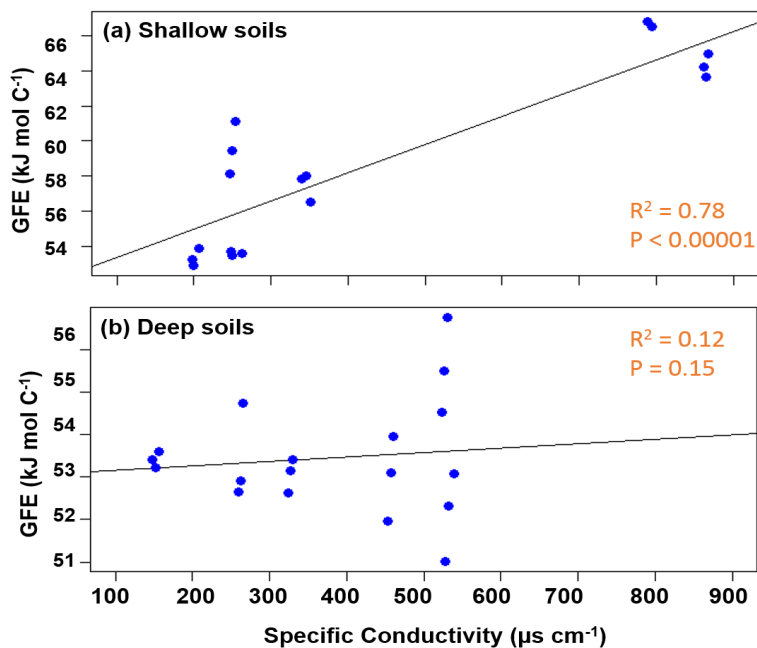
Site/Depth	Landscape position	Protein	Amino Sugar	Lipid	Lignin	Con HC	Tannin	Other	Carb	Unsat HC
BC2_Shallow	Fp	17.2	3.3	9.4	31.0	22.3	13.2	0.5	1.8	1.3
BC3_Shallow	Fp	21.6	3.8	11.5	27.3	23.0	9.8	0.4	1.5	1.2
BC4_Shallow	I	1.6	0.6	0.3	45.3	32.2	18.9	0.04	0.8	0.2
BC12_Shallow	Fp	7.6	1.8	4.0	38.1	31.2	15.3	0.1	1.2	0.7
BC13_Shallow	Fp	13.3	2.6	5.9	33.4	28.6	14.4	0.2	0.9	1.0
BC14_Shallow	I	6.1	1.7	1.6	37.0	35.8	16.	0.2	0.8	0.5
BC15_Shallow	U	3.7	1.5	1.3	51.8	18.5	21.0	0.2	1.5	0.5
BC2_Deep	Fp	2.3	0.5	1.5	41.2	27.2	25.7	0.2	1.1	0.3
BC3_Deep	Fp	3.2	0.3	3.1	34.1	33.4	24.4	0.3	0.9	0.2
BC4_Deep	I	2.8	0.8	0.6	50.4	27.7	16.5	0.2	0.7	0.2
BC12_Deep	Fp	2.29	0.40	1.43	43.3	27.9	22.9	0.2	1.2	0.3
BC13_Deep	Fp	3.47	0.62	2.00	39.8	33.6	19.2	0.2	0.8	0.3
BC14_Deep	I	1.71	0.76	0.57	43.7	32.5	19.34	0.2	1.0	0.2
BC15_Deep	U	9.51	2.55	4.70	63.8	5.1	9.93	0.7	1.0	2.6

1053



1054

1055 **Figure 1.** Study site Beaver Creek in the Olympic Peninsula in western Washington. The creek  
1056 is a first order stream with tidal exchange restored in 2014. Top panel shows site location in  
1057 western Washington with inset panel zoomed in to show site close to Johns River. Bottom panel  
1058 shows soil sampling locations at the high salt exposure (BC2, BC3, BC4) transect, moderate salt  
1059 exposure (BC12, BC13, BC14) transect, and terrestrial upland (BC15) site. The transects with  
1060 six sampling sites experience periodic inundation episodes which result in surface pooling of  
1061 tidal water. Map was created using ArcGIS 10.5 software (ESRI, 2017). Coordinate System:  
1062 GCS WGS 1984.



1063

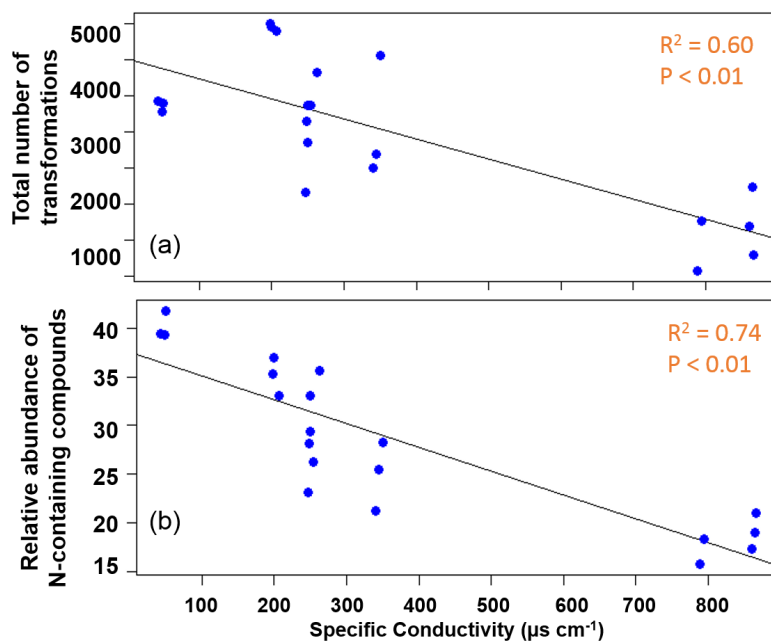
1064 **Figure 2.** Average Gibbs Free Energy (GFE) of samples in the water fraction of shallow soils  
1065 increased with increasing specific conductivity (a) while no change was observed in the deeper  
1066 soils (b).

1067

1068

1069

1070



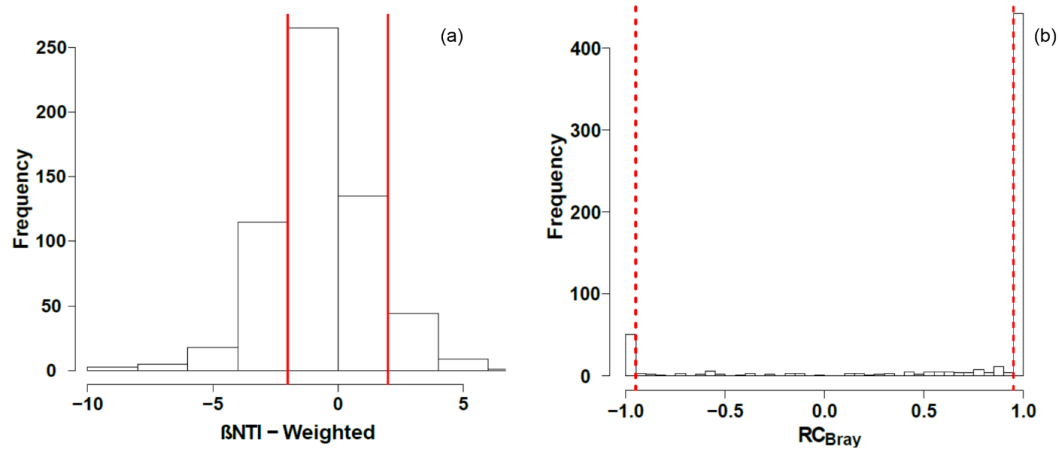
1071

1072 **Figure 3.** The total number of inferred transformations (a) and total abundance of N-containing  
1073 compounds (b) in the water fraction of shallow soils show significant negative correlations with  
1074 increasing specific conductivity. No significant relationships were observed for water fraction of  
1075 deeper soils or for the  $\text{CHCl}_3$  fraction in shallow or deeper soils.

1076

1077

1078



1079

1080 **Figure 4.** Histograms representing the observed distribution of comparisons based on (a) Beta-  
1081 near taxon index ( $\beta$ NTI) and (b) Raup Crick metric ( $RC_{\text{Bray}}$ ). Red lines represent the significance  
1082 thresholds, whereby values outside their bounds are significantly different from the null  
1083 distribution.

1084